BBA - Molecular Basis of Disease 1865 (2019) 2736–2752

Contents lists available at ScienceDirect

BBA - Molecular Basis of Disease

journal homepage: www.elsevier.com/locate/bbadis

Cardiomyocyte targeted overexpression of IGF1 during detraining restores compromised cardiac condition via mTORC2 mediated switching of PKCδ to PKCα

Emeli Chatterjee, Ratul Datta Chaudhuri, Sagartirtha Sarkar*

Genetics and Molecular Cardiology Laboratory, Department of Zoology, University of Calcutta, 35 Ballygunge Circular Road, Kolkata 700019, West Bengal, India

ARTICLE INFO

Keywords:
Exercise
Detraining
IGF1
mTORC2
PKCα
PKCδ

ABSTRACT

Altered cardiac adaptation of physiologically hypertrophied heart during detraining remained obscure for long time. We had previously reported the switching of protein kinase C (PKC) isoforms (-α to -δ) associated with functional deterioration of heart at detraining in mice undergone swim exercise. Here we report that, myocardium targeted overexpression of insulin-like growth factor 1 (IGF1) and knockdown of insulin-like growth factor 1 receptor (IGF1R) during detraining and exercise respectively altered the activation of PKCs and eventual cardiac condition. Moreover, downregulation of mammalian target of rapamycin complex 2 (mTORC2) was recorded in both IGF1R knockdown or detraining groups. Additionally, knocking down of mTORC2 during exercise exhibited impaired cardiac condition. Interestingly, significantly increased interactions of mTORC2 with both PKCα and δ was recorded exclusively in exercise group. This interaction resulted into hydrophobic motif phosphorylation of both PKCs (Serine657-PKCα; Serine662-PKCδ). Serine phosphorylation on one hand activated PKCα mediated cell survival and on the other hand alleviated the apoptotic activity of PKCδ during exercise. Mutation of Serine662 of PKCδ in exercised mice showed higher Tyrosine311 phosphorylation with increased apoptotic load similar to that in detrained animals. These observations confirmed that differential and conditional activation of PKCs depend upon IGF1 induced mTORC2 activation. Furthermore, blocking of PKCα resulted in activated p53 which in turn repressed IGF1 expression during swim, mimicking the condition of detrained heart. In conclusion, this is the first report to unravel the intricate molecular mechanism of switching a physiologically hypertrophied heart to a pathologically hypertrophied heart during exercise withdrawal.

1. Introduction

The beneficial role of exercise for good health and the detrimental effects of physical inactivity is well known and widely accepted [1–4]. A variety of scientific studies have shown that regimented endurance training fosters overall cardiac performance [1,5,6]. As a result of long-term exercise training, an “athlete's heart” [7] undergoes physiological hypertrophy, characterized by increased ventricular wall thickness together with enlarged ventricular chamber dimension [8], that results in enhanced efficiency and augmented cardiac functioning [5,9,10]. However, studies have shown that, athletes' hearts at exercise cessation encounter detraining effects [11] which are defined by complete or partial loss of long-term exercise-induced anatomical, physiological, and performance adaptations [12–15].

Protein kinase C (PKC) isoforms, a class of phospholipid dependent serine/threonine kinases are activated by second messenger [16]. Several reports have suggested that activation of PKCs is associated with an array of adaptive and maladaptive cardiac response [17,18].

Abbreviations: anf, atrial natriuretic factor; *β-mhc, β- myosin heavy chain*; *igf1, insulin like growth factor 1*; *α-mhc, α-myosin heavy chain*; *serca, sarco/endoplasmic reticulum Ca^{2+} ATPase*; *rpl32, 60S ribosomal protein L32*; BOC_2O, Di-tert-butyl dicarbonate; EDC, 1-ethyl-3-(3-dimethylaminopropyl) carbodiimide; NHS, N-hydroxysuccinimide; DLS, Dynamic light scattering; IGF1R, Insulin like growth factor 1 receptor; PKC, Protein kinase C; mTOR, Mammalian target of rapamycin; mTORC1, mTOR complex 1; mTORC2, mTOR complex 2; Akt, Protein kinase B; PARP, Poly ADP ribose polymerase; MDM, Mouse double minute 2 homolog; ERK, Extracellular signal-regulated kinases; His, Histidine; Ser, Serine; Tyr, Tyrosine; Thr, Threonine; RPL32, 60S ribosomal protein L32; CSA, Cross sectional area; CMC, Stearic acid modified carboxymethyl chitosan; CMCP, CMC conjugated to a 20-mer myocyte-targeted peptide; PBS, Phosphate buffered saline; IVST, Inter ventricular septum thickness; LVDD, left ventricular diastolic diameter; %FS, Percentage fractional shortening; RT, Reverse transcription; PCR, Polymerase chain reaction; SDS, Sodium dodecyl sulphate; PAGE, Polyacrylamide gel electrophoresis; PVDF, Polyvinyledine difluoride

* Corresponding author.
E-mail address: sagartirtha.sarkar@gmail.com (S. Sarkar).

https://doi.org/10.1016/j.bbadis.2019.07.003
Received 18 March 2019; Received in revised form 22 June 2019; Accepted 6 July 2019
Available online 09 July 2019

Our laboratory has previously shown that the switching of activation from PKCα to PKCδ isoform is associated with a compromised cardiac function in mice that were withdrawn from chronic exercise period [19], effectively transforming a 'good heart' into a 'bad heart'. Exclusive activation of PKCα was coupled with the swim exercise regimen, whereas PKCδ was significantly induced during the detraining period and was connected with pathological condition. Activated PKCα, during physiological hypertrophy promoted cardiomyocyte growth with upregulation of cell survival markers like protein kinase B (Akt), extracellular signal-regulated kinases (ERK) and decreased cellular apoptotic load resulting in improved cardiac function whereas, PKCδ activation, during detraining period resulted in activation of pro-apoptotic molecule p53 and other apoptosis markers in myocytes leading to impaired cardiac function.

Insulin like growth factor 1 (IGF1) and its receptor tyrosine kinase (IGF1R) regulate contractility, metabolism, hypertrophy, autophagy, senescence, and apoptosis in the heart [20,21]. Several studies have linked IGF1 with exercise-induced physiological cardiac hypertrophy [22–25] whereas others linked the shortfall of IGF1 to increased risk of cardiovascular diseases and mortality [21,26]. IGF1/IGF1R activates multiple downstream molecules including PKCs [27] and another serine/threonine protein kinase, the mammalian target of rapamycin (mTOR) [28,29]. mTOR is found in two structural and functional complexes (mTORC1 and mTORC2) with unique binding partners, namely, raptor and rictor for mTORC1 [30,31] and mTORC2 [32,33] respectively. mTORC2 is reported to phosphorylate PKCα [34], triggering downstream cell survival pathway [34,35]. However, IGF1-induced mTORC2-mediated regulation of PKCδ activation, leading to altered activity of pro-apoptotic molecule p53 is not well studied.

Therefore, the present study is designed to investigate the possible modulators involved in the transition of physiologically hypertrophied heart to a maladaptive heart during exercise withdrawal, in light of the differentially activated PKC isoforms (-α and -δ) involving IGF1 via mTORC2. A plausible contribution of active p53 to the disruption of the IGF1 signaling axis that culminates into a compromised cardiac fate during exercise withdrawal has also been addressed in this study for the first time.

2. Material and methods

2.1. Animals used

24 weeks-old Balb/c mice (*Mus musculus*) used in this study were acquired from National Institute of Nutrition, Hyderabad, AP, India. The investigation complies with the Guidelines for the Care and use of Laboratory Animals published by the US National Institute of Health (NIH Publication No.85-23, revised 1996) and was approved by the Institutional Animal Ethics Committee University of Calcutta (Registration #885/ac/05/CPCSEA) registered under "Committee for the Purpose of Control and supervision of Experiments on Laboratory Animals" (CPCSEA), Ministry of Environment and Forests, Government of India.

2.2. Generation of animal models

Male Balb/c mice ($n = 5$ for each group) were used to generate different models for this study. Physiological hypertrophy was generated via swim exercise training for 4 weeks as described earlier [10,19,36] with few modifications (group S). Briefly, mice were allowed to swim daily for 60 min (twice daily for 30 min duration) for 4 weeks in a water chamber (100 cm in length, 60 cm in width and 50 cm in height) whose temperature was maintained at 30°C. Mice were accustomed to the swim exercise routine progressively from 10 min twice daily with increments of 10 min/day. Another group (D), first underwent swim exercise for 4 weeks and was then maintained for more 2 weeks at detraining condition as described previously [19]. 24 weeks old sedentary mice were used as control group (C). Animals were maintained on standard mice chow and water ad libitum in a climate controlled, light-regulated space with 12-hour light and dark cycles at the Institutional animal facility of the University of Calcutta. All experimental groups were sacrificed after the treatment period and cardiac tissues were processed accordingly for different experiments. Hypertrophy was measured from the heart weight (HW; in milligrams)-to-body weight (BW; in grams) ratio (HW/BW) [37].

2.3. Plasmid construction

Full length coding DNA sequence of mouse *igf1*(GenBank: AF440694.1) and Wild type *pkcδ* (GenBank: AY545076.1) with C-terminal his-tag were cloned in frame into pcDNA6/V5-his B mammalian expression vector separately (Thermo-fisher, USA), as described previously [38]. Briefly, RNA was extracted from *Mus musculus* heart tissue and cDNAs were prepared from the RNA by reverse transcription (RT)-PCR followed by PCR with respective primer sets (Supplementary Table 1) having specific restriction sites. All the clones were confirmed by sequencing (Applied Biosystems 3730, DNA analyzer). A mutant PKCδ pcDNA was constructed that contains the hydrophobic motif (HM: Serine662) mutation substituted by Alanine. The mutation was introduced into the pkcδ wild type pcDNA by polymerase chain reaction (PCR) based oligonucleotide-mediated Quik Change site-directed mutagenesis kit (Agilent Technologies, USA). The incorporation of the Alanine was performed by using respective primers and confirmed by cycle sequencing.

2.4. Preparation and characterization of myocyte-targeted gene delivery system in vivo

Stearic acid modified carboxymethyl chitosan (CMC) was prepared from low molecular weight Chitosan (Sigma-Aldrich, USA) and modified by Di-tert-butyl dicarbonate (BOC_2O) before conjugation to a cardiomyocyte specific 20-mer peptide (WLSEAGPVVTVRALRGTGSW) by 1-ethyl-3-(3-dimethylaminopropyl) carbodiimide (EDC) - N-hydroxysuccinimide (NHS) (Thermo Fisher, USA) as described earlier [39]. Trifluoroacetic acid (Sigma-Aldrich, USA) was used for BOC_2O removal. IGF1R siRNA, rictor siRNA, p53 siRNA, non-specific siRNA (Qiagen, Germany), empty plasmid and plasmids encoding IGF1, wild type and mutant PKCδ cloned in pcDNA6/V5-His B mammalian expression vector were added to CMC-peptide (CMCP) at different weight ratios and incubated for 2 h at 4 °C under constant shaking condition (400 rpm) Finally, nanoconstructs were filtered and lyophilized. CMCP encapsulated Plasmids/siRNAs were biophysically characterized by DLS (dynamic light scattering) (DynaProNanoStar™; Wyatt Technology, USA), ζ potential (Mo¨biufζ™ Mobility Instrument; Wyatt Technology, USA) as described earlier [39,40].

2.5. Treatment with cardiac gene delivery system

Plasmids with CMCP were intravenously injected via tail vein to D group of mice for overexpression of IGF1wild type construct (group D^{IO}). S group of mice were similarly administered with PKCδ wild type (S^{WT}) and mutant (S^{M}) constructs. S group of mice were administered with IGF1R siRNA-CMCP (S^{I}) and rictor siRNA-CMCP (S^{R}) whereas, D group was treated with p53 siRNA-CMCP. Treatment with plasmids/siRNA in group D was continued from 10th till last day of the resting period whereas, treatment of S group continued from the 10th day of exercise period on alternate days till the last day of exercise. Both overexpression plasmids as well as siRNAs were administered at a dose of 2 mg/kg of BW/day. Mice treated with empty plasmid-CMCP or non-specific siRNA (NS siRNA; Allstars Negative Control Qiagen, Germany) with CMCP were used as respective controls for subsequent experiments. Heart, kidney, brain, liver and lung tissues were collected for further experimentation.

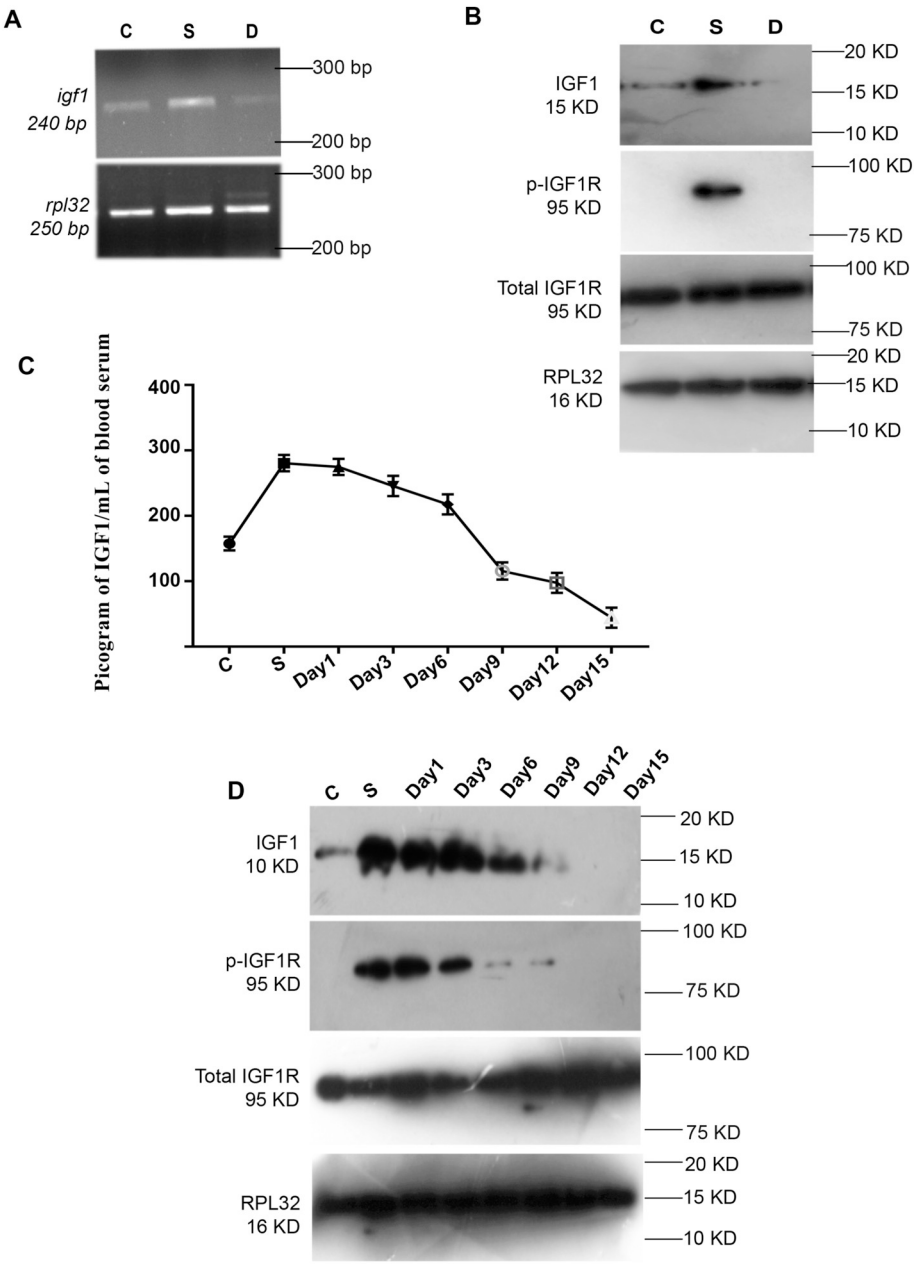

Fig. 1. Downregulation of IGF1/IGF1R during detraining. (A) RT-PCR analysis showing changes in expression of *igf1* among different experimental groups. *rpl32* was used as internal loading control. (B) Representative western blots showing changes in expression of IGF1 and phospho/total IGF1R among different experimental groups with RPL32 as internal loading control. (C) Graphical representation of IGF1 ELISA showing time-dependent downregulation of serum IGF1 concentration in blood samples of exercised animals detrained for different time periods compared to that of either S or C. (D) Western blot analyses showing a time-dependent change in expression of IGF1 and phospho/total IGF1R in exercised animals detrained for different time periods. RPL32 was used as internal loading control. S: exercise trained mice; D: detrained mice; C: sedentary control. All experiments were repeated independently for three times and the graphical representation was expressed as mean(±.S.E) of three independent experiments.

2.6. Treatment with chemical inhibitor against PKCα and PKCδ

PKCα specific chemical inhibitor Go¨6976 (Sigma-Aldrich, USA) and PKCδ specific chemical inhibitor Rottlerin (Sigma-Aldrich, USA) were dissolved in DMSO. S and D groups of mice were administered with respective PKCα and PKCδ inhibitors in 1X PBS intraperitoneally at a dose of 600 μg/day/kg body weight during the last seven days of the experimental period as described earlier [19]. Respective control mice were injected with 1X PBS during the experimental tenure.

2.7. Histology

2.7.1. Haematoxylin/Eosin staining

Hearts were taken out and washed in 1X PBS, fixed in Karnovsky's fixative, as described earlier [41]. Paraffin embedded tissues were cut into 4 μm sections and sections were processed and stained with haematoxylin/eosin (H/E). Cardiomyocyte cross-sectional areas (CSA) from each sample were quantified by using a computer morphometric program (ImageJ, NIH).

2.7.2. Masson's trichrome staining

Mice ventricular coronal tissue sections (4–5 μm) were taken to estimate the percentage of collagen volume fraction (%CVF). Tissue sections were stained with Masson's trichrome staining reagent (Sigma-Aldrich, USA) and collagen deposition were analysed under microscope (Nikon NIS BR) (Nikon, Shinagawa, Tokyo, Japan) following standard protocol. Digitization and processing of the captured images were done by using a computer morphometric program (ImageJ, NIH). Collagen volume fraction was calculated as the sum of all collagen stained tissue areas of the coronal sections represented as percentage (%) of the total surface area of the section [39].

2.8. Reverse transcriptase PCR (RT-PCR)

Total RNA was isolated from left ventricular heart tissues of each experimental groups using TriZol reagent (Invitrogen) following manufacturer's protocol. Expression of *igf1*, pathological hypertrophy marker genes [*atrial natriuretic factor* (*anf*), *β-myosin heavy chain* (*β-mhc*)] and physiological hypertrophy marker genes [*α-myosin heavy*

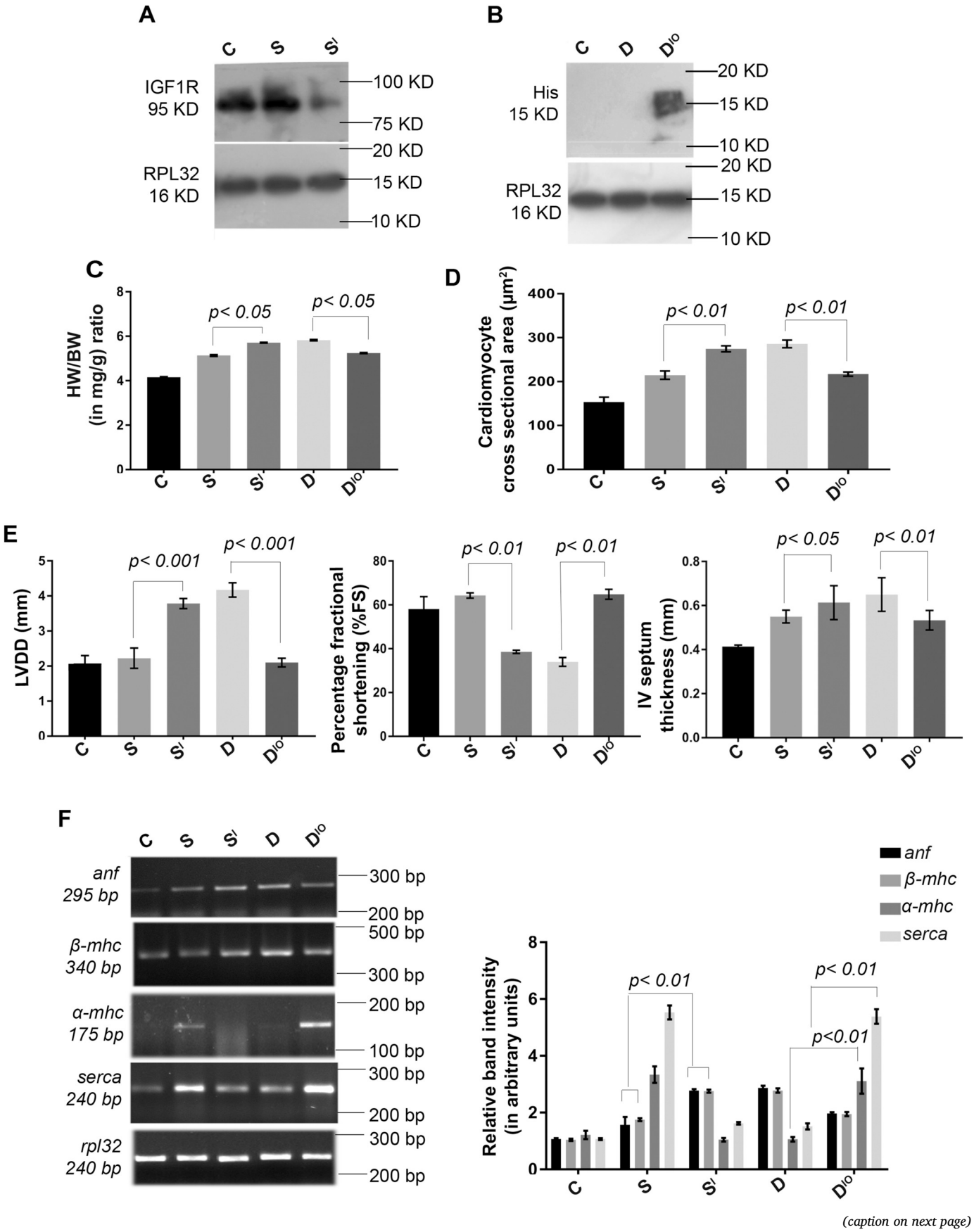

(caption on next page)

Fig. 2. Myocardium targeted overexpression and blocking of IGF1/IGF1R alters cardiac condition. (A) Representative western blot showing significant down-regulation of IGF1R expression in S^I compared to S. RPL32 was used as internal loading control. (B) Immunoblotting with anti-his antibody showing overexpression of IGF1 in D^{IO} compared to D and RPL32 was used as internal loading control. (C) Graphical representation of significant increase in HW/BW ratios in S^I compared to S and decrease in D^{IO} compared to D. (D) Graph showing changes in CSA (in μm^2) in different experimental groups. (E) Graphs showing significantly increased LVDD, IVST in S^I compared to S and increased %FS in D^{IO} compared to D. (F) RT-PCR analysis showing significantly increased expression of *anf* and *β-mhc* in S^I compared to S, *α-mhc* and *serca* in D^{IO} compared D. *rpl32* was used as loading control. Corresponding graph showing relative fold changes in gene expression of different hypertrophy markers. S: exercise trained mice treated with NS siRNA/empty plasmid-CMCP; S^I: exercised trained mice treated with myocyte targeted IGF1R siRNA-CMCP; D: detrained mice treated with NS siRNA/empty plasmid-CMCP; D^{IO}: myocyte targeted IGF1 overexpressed D mice; C: control mice treated with NS siRNA/empty plasmid-CMCP. All experiments were repeated independently for three times and the graphical representations were expressed as mean (±S.E.) of three experiments.

chain (*α-mhc*), *sarco/endoplasmic reticulum* Ca^{2+}*ATPase* (*serca*)], *collagen1* (*col1*), *collagen3* (*col3*) *60S ribosomal protein L-32* (*rpl32*) as internal loading control were checked using respective forward and reverse primers (Supplementary Table 1).

2.9. Protein extraction

Protein from hearts of all experimental groups was isolated using M-PER Mammalian protein extraction reagent (Thermo Scientific, USA) according to the manufacturer's protocol. Protein extracts were prepared from ventricular tissues using previously described procedure [42]. Membrane fractions from tissue samples were isolated using Mem-per plus membrane protein extraction kit (Thermo Scientific, USA) using the manufacturer's protocol.

2.10. Western blotting

Western blot analysis was done as described previously [41]. Briefly, 40 μg and 200 μg protein samples were separated in SDS-PAGE for total and phospho proteins respectively and transferred to PVDF + membrane (Millipore, Billerica, USA). Membranes were blocked with 5% nonfat dry milk followed by incubation with primary antibodies to IGF1, PKCα, phospho-PKCα (Ser657) (Abcam, UK); IGF1R, phospho-IGF1R (Tyr1135), rictor, mTOR, phospho-mTOR (Ser2481), Akt, phospho-Akt (Ser473), p53, phospho-p53 (Ser15, Ser46),caspase-3, PARP, PKCδ, phospho-PKCδ (Tyr311) (Cell Signaling, USA); phospho-PKCδ (Ser662) (Santa Cruz Biotechnology, USA) and appropriate HRP-conjugated secondary antibodies (Pierce, USA). Immunoreactive bands were visualized by enhanced chemiluminescence kit (Millipore, USA). RPL32 (Abcam, UK) was used as loading control for cytosolic proteins. A major band from a Coomassie blue stained SDS-PAGE gel of fractionated membrane proteins was used as a loading control for membrane protein fractions. All blots were normalized by respective loading controls. The blots were scanned and quantitated using the GelDoc XR system and Quantity One® software version 4.6.3 (Bio-Rad, USA).

2.11. Estimation of IGF1 in blood serum

The amounts of circulating IGF1 in blood serum of different experimental groups with increasing period of detraining (day 1–15 post exercise) were estimated using respective ELISA kit (RayBiotech, USA) following the manufacturers' protocol. Results were expressed as the number of picograms of IGF1 per millilitre of blood serum.

2.12. Co-immunoprecipitation

Co-immunoprecipitation was done following the manufacturer's protocol (Pierce Co-Immunoprecipitation Kit, USA). Briefly, proteins were incubated with fast flow protein G or protein A Sepharose beads and centrifuged to eliminate non-specifically bound proteins. Concentration of the precleared proteins was estimated by Bradford's Assay. 200 μg of proteins were immunoprecipitated using primary antibody of anti-mTOR (Cell Signaling, USA). The immune-protein complexes were again incubated with protein G or protein A Sepharose beads. Attached proteins were eluted from the beads in 1% SDS buffer followed by immunoblotting with antibodies against PKCα (Abcam, UK); PKCδ, rictor, mTOR (Cell Signaling, USA) [38]. Normalization was done by immunoblotting using the same antibodies used to immunoprecipitate the proteins.

2.13. Determination of cardiac function by M-mode echocardiography

Two-dimensional echocardiography was performed to determine cardiac function using an ultrasound system (Vivid S5 system, GE Healthcare, USA) as described earlier [43]. M-mode views of the parasternal short axis of left ventricle was assessed to measure the left ventricular diastolic diameter (LVDD), fractional shortening (% FS), inter ventricular septum thickness (IVST).

2.14. Statistical analysis

All results were expressed as mean (±S.E) of three independent experiments. Data were analysed by independent sample *t*-test (for comparison of two groups) and ANOVA followed by Tukey's test (for multiple groups comparison) using GraphPad Prism (Version 7.0, GraphPad Software, USA). Results with p-value < 0.05 were considered significant.

2.15. Key resources table

Resource	Source	Identifier
Antibodies		
IGF1, PKCa, phospho-PKCa (Ser657), RP-L32	Abcam	N/A
IGF1R, phospho-IGF1R (Tyr1135), rictor, mTOR, phospho-mTOR (Ser2481), Akt, phospho-Akt (Ser473), p53, phospho-p53 (Ser15, Ser46),caspase-3, PARP, PKCd, phospho-PKCd (Tyr311),	Cell Signaling	N/A
phospho-PKCd (Ser662)	Santa Cruz Biotechnology	N/A
Chemical		
Go¨6976, Rottlerin	Sigma Aldrich	N/A
IGF1 ELISA Kit	RayBiotech	N/A
Quik Change site-directed mutagenesis kit	Agilent Technologies	N/A
siRNAs against IGF1R, rictor, p53	Qiagen	N/A
Experimental organism		
Mus musculus	National Institute of Nutrition, Hyderabad, AP, India	N/A

3. Results

3.1. Downregulated expression of IGF1 is associated with transition from physiological hypertrophy to cardiac deterioration during detraining

Generation of physiological hypertrophy in swim group (S) was confirmed by significantly increased heart weight to body weight ratio (HW/BW), cardiomyocyte cross sectional area (CSA), physiological hypertrophy markers *α-mhc* and *serca* compared to sedentary control group (C) (Supplementary Fig. 1A, B, D). M-mode echocardiography analysis revealed marked increase in left ventricular diastolic diameter

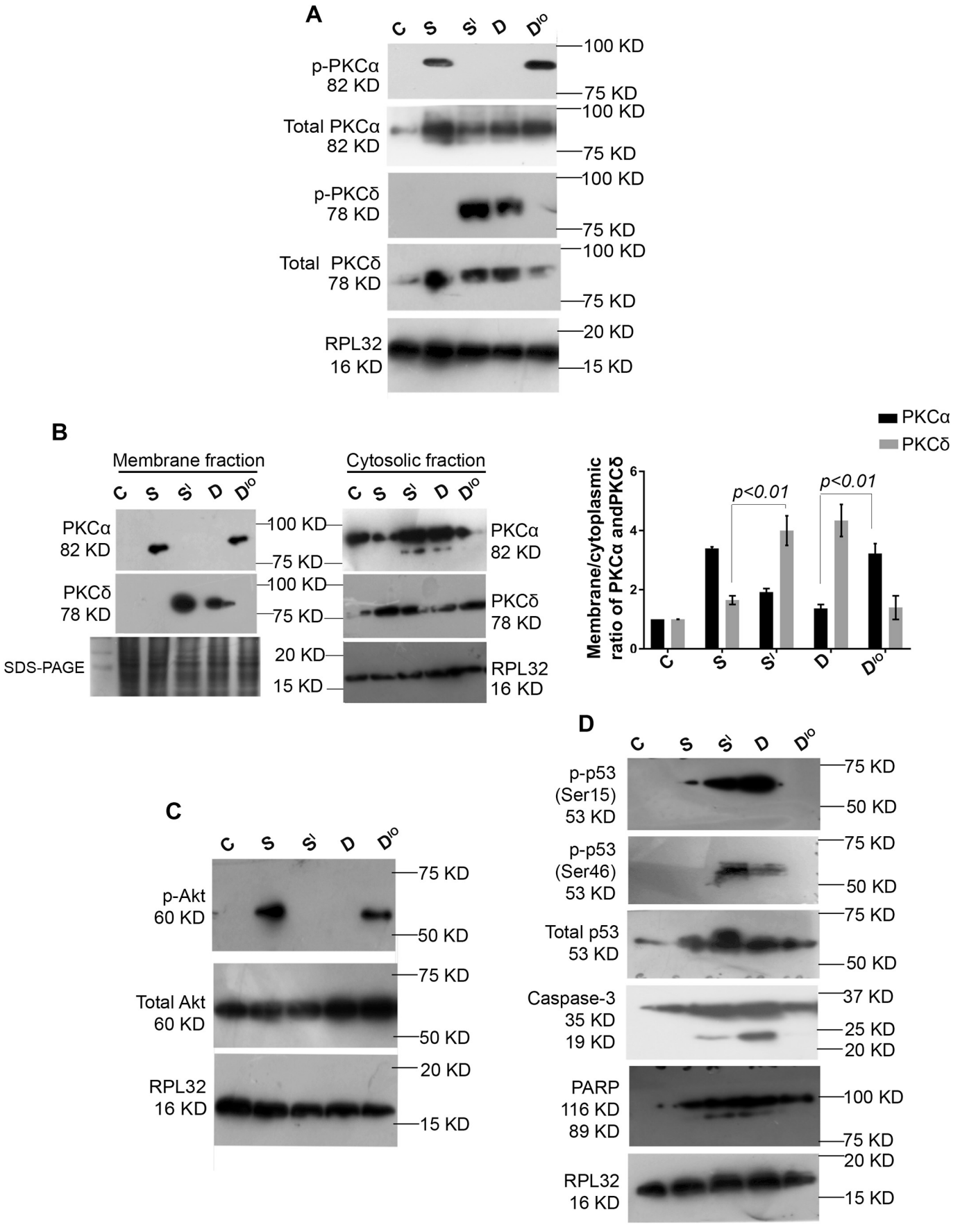

(caption on next page)

Fig. 3. Myocardium targeted overexpression and blocking of IGF1/IG1R alters PKCs activation. (A) Representative western blots showing significantly increased phospho/total ratio of PKCα in D^{IO} compared to D and significantly increased phospho/total ratio of PKCδ in S^{I} compared to S. RPL32 was used as internal loading control. (B) PKCα and PKCδ also showed differential expression in membrane/cytoplasmic fractions among different treatment groups. A major band from a Coomassie blue stained SDS-PAGE gel of fractionated membrane proteins and RPL32 for cytoplasmic proteins were used as internal loading controls. Corresponding graphical representation showing significantly increased expression of membranal/cytoplasmic PKCα in D^{IO} compared to D and PKCδ in S^{I} compared to S. (C) Representative western blots showing phosphorylation of Akt only in D^{IO} and S. (D) Representative western blots showing significantly increased phospho/total p53 (Ser15, Ser46), cleaved Caspase-3 and PARP in S^{I} compared to S. RPL32 was used as internal loading control. S: exercise trained mice treated with NS siRNA/empty plasmid-CMCP; S^{I}: exercised trained mice treated with myocyte targeted IGF1R siRNA-CMCP; D: detrained mice treated with NS siRNA/empty plasmid- CMCP; D^{IO}: myocyte targeted IGF1 overexpressed D mice; C: control mice treated with NS siRNA/empty plasmid-CMCP. All experiments were repeated independently for three times and the graph was expressed as mean (±S.E.) of three experiments.

(LVDD: 2.65 ± 0.021 mm), fractional shortening (%FS: 64.3 ± 1.172%) and inter-ventricular septum thickness (IVST: 0.55 ± 0.02 mm) in S group compared to C (LVDD: 2.03 ± 0.09%FS: 58.07 ± 5.64%; IVST: 0.41 ± 0.006 mm; Supplementary Fig. 1C).

However, compromised cardiac condition was evident in detraining group (D) characterized by significantly increased HW/BW, CSA and increased expression of pathological hypertrophy marker genes *anf*, *β-mhc* (Supplementary Fig. 1A, B, D) with significantly reduced expression of *α-mhc* and *serca* compared to S group (Supplementary Fig. 1D). Significantly compromised cardiac function was evident in group D mice (increased LVDD 3.897 ± 0.06 mm; IVST 0.66 ± 0.005 mm and decreased %FS 35.23 ± 2.62%; Supplementary Fig. 1C) compared to either group C or S.

Significant upregulation of *igf1* expression was observed in S group (3.06 ± 0.18-fold) compared to group C (Fig. 1A). On the contrary, group D showed significant downregulation of *igf1* expression compared to group C (1.87 ± 0.76-fold) and S (2.568 ± 0.845-fold) (Fig. 1A). Similar trend was observed in expression of IGF1 protein among three experimental groups (5.608 ± 0.44-fold induction in group S compared to C and 3.75 ± 0.71-fold downregulation in D group compared to group C) (Fig. 1B). Phosphorylation of IGF1R showed marked decrease in D group (3.809 ± 0.24-fold) compared to S group further corroborating earlier trend (Fig. 1B).

Time point study (1 to 15 days post exercise) revealed gradual decrease in serum IGF1 level with increasing period of detraining in S group of animals (day 1: 274.9 ± 7.101 pg/ml, day 3: 245.7 ± 8.945 pg/ml, day 6: 217.5 ± 8.813 pg/ml, day 9: 115.6 ± 7.645 pg/ml, day 12: 97.49 ± 8.841 pg/ml, day 15: 44.22 ± 8.89 pg/ml) compared to group S (280.6 ± 7.226 pg/ml) and decrease from day 9 onwards when compared to group C (157.7 ± 6.15 pg/ml) (Fig. 1C). Similar time point detraining study in group S animals (1–15 days post exercise) revealed gradual downregulation of IGF1 protein expression compared to S group (day 3: 1.12 ± 0.12-fold, day 6: 2.187 ± 0.0528-fold, day 9: 3.12 ± 0.23-fold, day 12: 3.924 ± 0.012-fold, day 15: 4.167 ± 0.078-fold) while phosphorylation of IGF1R was detected till 3rd day of detraining (Fig. 1D).

3.2. Reversal of cardiac fate by myocardium-targeted knocking down of IGF1R during exercise training and overexpression of IGF1 during detraining

Significant knockdown of total IGF1R expression was observed in ventricular tissue of S group of mice administered with IGF1R siRNA-CMCP (group S^{I}: 3.09 ± 0.12fold) compared to non-specific siRNA (NS siRNA-CMCP) treated S group (Fig. 2A). Further, cardiac tissue specific knockdown of IGF1R was confirmed by downregulated expression of IGF1R in heart tissue compared with bystander organs of S^{I} group (Supplementary Fig. 2A). On the other hand, immunoblotting using anti-Histidine, 'his' antibody showed successful over expression of IGF1 in D group of mice treated with IGF1-CMCP (group D^{IO}: 3.12 ± 0.23-fold) compared to empty plasmid-CMCP treated group D (Fig. 2B). Furthermore, mice with overexpressed IGF1-CMCP showed higher cardiac tissue-specific expression of 'his' compared with other organs (Supplementary Fig. 2B).

Interestingly, HW/BW was significantly increased in both group S^{I} and group D (group S^{I}: 5.712 ± 0.018; group D: 5.82 ± 0.028) compared to group S (5.136 ± 0.03) and D^{IO} (5.24 ± 0.02 Fig. 2C). Marked increase in CSA was observed in groups S^{I} and D (group S^{I}: 274.6 ± 3.02 μm^2; group D: 285.8 ± 3.89 μm^2) compared to either group S (214.6 ± 4.238 μm^2) and D^{IO} (217.4 ± 2.09 μm^2, Fig. 2D). Significantly upregulated expression of pathological hypertrophy markers *anf*, *β-mhc* were evident in group S^{I} (*anf*: 1.588 ± 0.006-fold; *β-mhc*: 1.508 ± 0.011-fold) compared to group S (Fig. 2F) as revealed by RT-PCR analysis. Moreover, *α-mhc* and *serca* showed significantly upregulated expressions in group D^{IO} (*α-mhc*: 2.925 ± 0.377-fold; *serca* 3.577 ± 0.25-fold) compared to D group (Fig. 2F). Collagen level was studied both at mRNA and protein levels in various groups that showed significantly upregulated expression of both *col1* (3.29 ± 0.10-fold) and *col3* (3.09 ± 0.20-fold) in group S^{I} along with significantly higher percentage of collagen volume fraction (%CVF) in group S^{I} (2.863 ± 0.202-fold) compared to group S as revealed by Masson's Trichrome staining (Supplementary Fig. 4A–B). Knockdown of total IGF1R in S^{I} group revealed compromised heart function with increased LVDD, IVST and decreased %FS (LVDD: 3.783 ± 0.14 mm; IVST: 0.61 ± 0.07 mm; %FS: 38.57 ± 1.17%) compared to group S (LVDD: 2.22 ± 0.28 mm; IVST: 0.55 ± 0.02%; %FS: 64.3 ± 1.17%) (Fig. 2E). On the other hand, group D^{IO} with IGF1 overexpression, revealed improved cardiac condition with decreased LVDD, IVST and restored %FS (LVDD: 2.15 ± 0.12 mm; IVST: 0.53 ± 0.04; %FS: 64.83 ± 2.24%) compared to D group (LVDD: 4.173 ± 0.20 mm; IVST: 0.65 ± 0.07 mm; %FS: 33.96 ± 2.02%) (Fig. 2E).

3.3. IGF1-mediated modulation of differential activation of PKCα, PKCδ and their downstream target proteins

IGF1-mediated regulation of PKCs were determined in all experimental groups. Interestingly, S^{I} showed significantly increased phospho/total PKCδ (2.64 ± 0.26-fold) similar to group D, when compared to group S (Fig. 3A). On the other hand, phospho/total PKCα was significantly upregulated in group D^{IO} (2.051 ± 0.09-fold) compared to D group (Fig. 3A). These findings were further corroborated by analysing membrane translocation of active PKCα from cytosol in D^{IO} and S groups and activated PKCδ in S^{I} and D groups respectively (Fig. 3B).

Phospho Akt (Ser473) was significantly higher in D^{IO} group (2.745 ± 0.36-fold) compared to group D (Fig. 3C), without any alteration of total Akt level among all the experimental groups (Fig. 3C). No phosphorylation of Akt was recorded in groups S^{I} and D (Fig. 3C).

Activation of p53 as a downstream pro-apoptotic molecule of PKCδ revealed significantly increased expression of both total and phospho p53 in groups S^{I} (total p53: 5.94 ± 0.22-fold; phospho p53: 3.05 ± 0.12-fold for Ser46; 3.72 ± 0.01-fold for Ser15) and group D (total p53: 5.67 ± 0.13-fold; phospho p53: 3.94 ± 0.02-fold for Ser46; 3.64 ± 0.01-fold for Ser15) when compared to group S (Fig. 3D). Cleaved product for caspase-3 and Poly ADP ribose polymerase (PARP) was evident in group S^{I}, similar to group D (Fig. 3D).

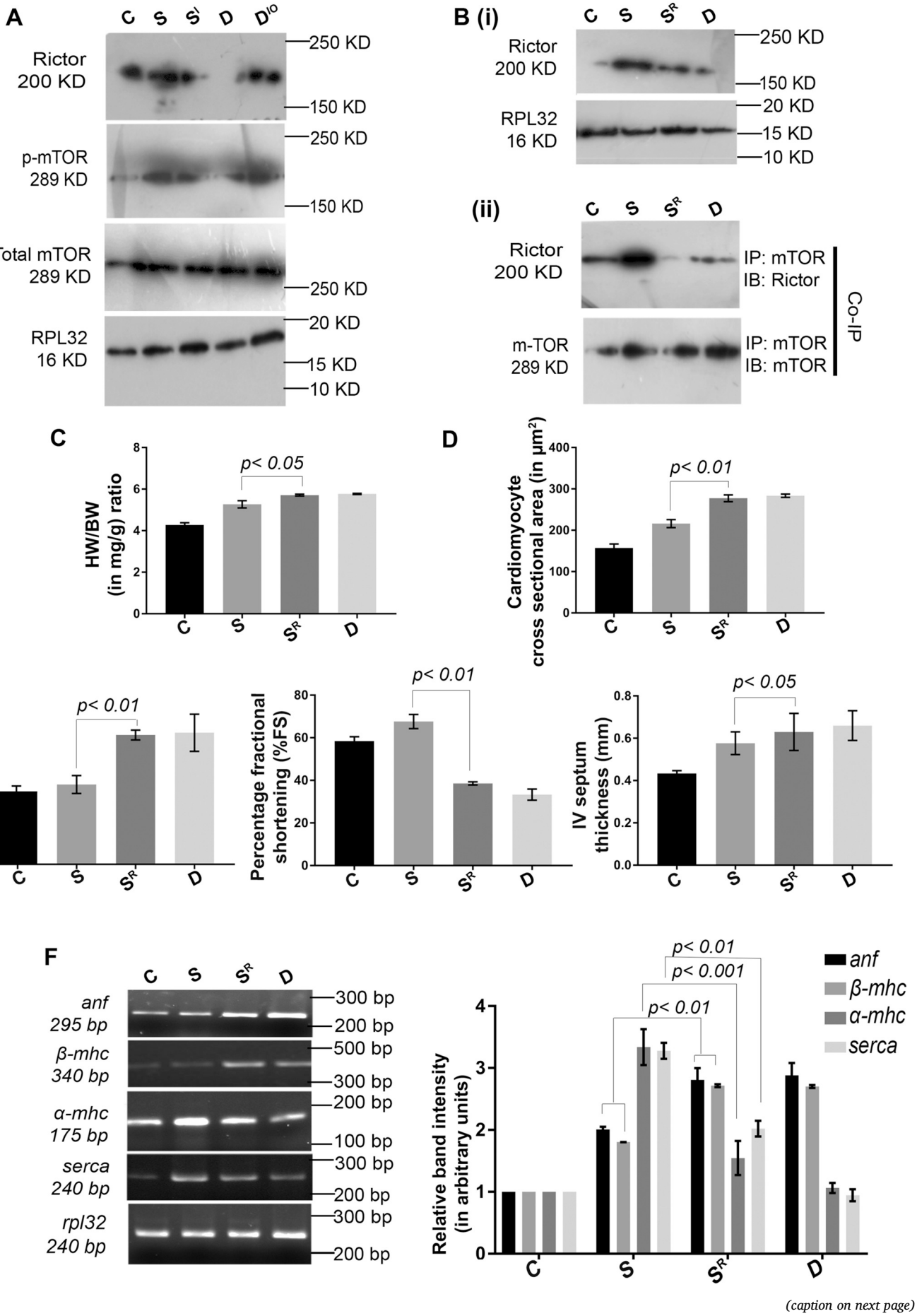

(caption on next page)

Fig. 4. Association of mTORC2 with IGF1 mediates physiological/pathological cardiac hypertrophy. (A) Representative western blots showing significantly increased expression of rictor, phospho-mTOR in D^{IO} compared to D, although total mTOR remained same in all experimental groups. RPL32 was used as internal loading control. (B) (i) Western blot analyses showing significantly downregulated expression of rictor in S^R compared S, using RPL32 as internal loading control; (ii) Co-immunoprecipitation analyses using anti-mTOR antibody followed by immunoblotting with anti-rictor antibody revealed downregulated interaction between mTOR and rictor in S^R compared to S. Blots were normalized by immunoblot of mTOR in the same samples. (C) Graph showing significant increase in HW/BW ratio in S^R compared to S. (D) Graphical representation of significantly increased CSA (in μm^2) in S^R compared to S. (E) Graphs showing marked increase in LVDD, IVST and decreased %FS in S^R compared to S. (F) RT-PCR analysis showing significantly increased expression of *anf* and *β-mhc* and decreased expression of *α-mhc* and *serca* in S^R compared to S. Corresponding graph showing expression profile of different hypertrophy markers. *rpl32* was used as internal loading control. S: exercised mice treated with NS siRNA/empty plasmid-CMCP; S^I: exercised trained mice treated with myocyte targeted IGF1R siRNA-CMCP; S^R: exercised mice treated with myocyte targeted rictor siRNA-CMCP; D^{IO}: myocyte targeted IGF1 overexpressed D mice D: detrained mice treated with NS siRNA/empty plasmid-CMCP; C: control mice treated with NS siRNA/empty plasmid-CMCP. All experiments were repeated independently for three times and the graphical representations were expressed as mean (±S.E.) of three experiments.

3.4. IGF1 in association with mTORC2, modulates the cardiac fate

3.4.1. IGF1 alters mTORC2 expression

The overall status of mTORC2 was checked by analysing the expression of rictor, mTORC2 specific phospho-mTOR (Ser2481) and total mTOR. Western blot analyses revealed significantly decreased expression of rictor in groups S^I and D (S^I: 4.325 ± 0.3-fold and D: 5.766 ± 0.35-fold) compared to group S (Fig. 4A). mTOR phosphorylation showed marked decrease in group S^I (2.99 ± 0.22-fold) compared to S group, similar to group D (Fig. 4A). However, D^{IO} group showed significant restoration of mTORC2 expression (4.73 ± 0.36-fold for rictor; 2.48 ± 0.10-fold for phospho-mTOR) compared to D group (Fig. 4A). No significant alteration in total mTOR was found in any experimental group (Fig. 4A).

3.4.2. mTORC2 dictates the altered cardiac fate

Myocardium-targeted delivery of rictor siRNA-CMCP (group S^R) in S group of mice hearts showed successful knockdown of rictor in group S^R (1.68 ± 0.01-fold) compared to S group [Fig. 4B (i)]. Western blot analysis revealed no significant change of rictor expression in bystander organs of S^R group (data not shown). Additionally, immunoprecipitation with anti-mTOR antibody succeeded by immunoblotting with anti-rictor antibody showed markedly lower interaction of rictor with mTOR in both S^R and D groups (3.52 ± 0.32-fold for S^R, 4.283 ± 0.38-fold for D) compared to S group [Fig. 4B (ii)]. Animals of S^R group showed significantly increased HW/BW ratio (5.712 ± 0.01) compared to group S (5.27 ± 0.07; Fig. 4C) akin to D group (5.768 ± 0.01; Fig. 4C). CSA was also significantly increased in group S^R (277.4 ± 3.682 μm^2) compared to group S (216.2 ± 4.29 $\mu m^{2)}$, similar to D group (283.6 ± 1.806 μm^2, Fig. 4D).

S^R group also showed attenuated cardiac efficacy as evidenced by significantly increased LVDD (3.783 ± 0.14 mm), IVST (0.63 ± 0.08 mm) and decreased %FS (38.57 ± 0.74%) compared to group S (LVDD: 2.33 ± 0.26 mm; IVST: 0.57 ± 0.05 mm; %FS: 67.63 ± 3.33%; Fig. 4E). rictor knockdown during physiological cardiac hypertrophy showed significant upregulation of pathological hypertrophy markers (*anf*: 1.505 ± 0.072-fold, *β-mhc*: 1.504 ± 0.014-fold) in S^R group when compared to S group, similar to group D (Fig. 4F). On the other hand, significant downregulation of *α-mhc* and *serca* was found in S^R group (*α-mhc*: 2.278 ± 0.381-fold, *serca*: 1.639 ± 0.137-fold) compared to group S, as was observed in D group (Fig. 4F).

3.5. mTORC2- a key regulator of heterogeneous regulation of PKCα and PKCδ activation during exercise and detraining

Co-immunoprecipitation experiments using anti-mTOR antibody followed by immunoblotting with anti-PKCα, anti-PKCδ and anti-rictor antibody showed significantly higher interaction of PKCα with mTOR in S group (4.306 ± 0.39-fold) compared to either groups S^R or D (Fig. 5A). Interestingly, PKCδ also showed significantly increased association with mTOR in S group (3.485 ± 0.27-fold) compared to both groups S^R and D (Fig. 5A). However, increased level of mTOR-bound rictor in group S (3.788 ± 0.29-fold) compared to both S^R group and D group was indicative of higher mTORC2 expression in group S (Fig. 5A). Activation status of both PKC isoforms (PKCα and PKCδ) in membrane protein fractions of the same tissue samples revealed induced plasma membrane translocation from cytosol of PKCα exclusively in group S and PKCδ in S^R/D groups of animals implicating activation of these PKC isoforms in respective groups (Fig. 5B). Intermediate phosphorylation events for PKCα (Ser657) and PKCδ [Hydrophobic motif (HM): Ser662; Tyr311] were checked via western blot analyses. PKCα phosphorylation (Ser657) was exclusively evident in S group (Fig. 5C). On the other hand, phosphorylation at Ser662 of PKCδ was solely recorded in S group whereas phosphorylation at Tyr311 of PKCδ was observed in both S^R and D groups but was absent in S group (Fig. 5C).

3.6. Hydrophobic motif deactivation results in higher PKCδ activation along with apoptotic regulators during detraining

Wild type and Ser662 deficient mutant of PKCδ (Alanine) cloned in pCDNA6/V5 His-B mammalian expression vector were encapsulated in CMCP for cardiac tissue targeted delivery in two separate swim groups. Western blot analysis using anti-his antibody showed successful over expression of wild type (S^{WT}) and mutant (S^M) PKCδ (Fig. 6A), abating bystander effects (data not shown).

Immunoblotting showed significantly reduced Ser662 phosphorylation level of PKCδ in groups S^M and D (S^M: 2.588 ± 0.19-fold and D: 2.975 ± 0.32-fold) compared to S^{WT} group (Fig. 6B). However, PKCδ HM mutation, induced Tyr311 phosphorylation level in groups S^M and D (group S^M: 4.093 ± 0.045-fold; group D: 4.26 ± 0.54-fold) compared to S^{WT} (Fig. 6B). No significant difference in phosphorylation (Ser662, Tyr311) of PKCδ was seen in S^{WT} and S groups (Fig. 6B). Significantly higher expression of active PKCδ in membrane fractions in S^M and D groups compared to S^{WT} and S groups was also recorded (Fig. 6C).

Western blot analyses revealed significantly increased phospho/total ratio of p53 in S^M (Ser15: 2.628 ± 0.16-fold; Ser46: 3.225 ± 0.27-fold) compared to S^{WT} group (Fig. 6D), akin to group D (Ser15: 2.734 ± 0.19-fold; Ser46 3.38 ± 0.43-fold). Cleaved products of PARP and caspase-3 proteins were also evident in S^M and D groups (Fig. 6D).

3.7. Conditional activation of PKC isoforms differentially regulates IGF1 via p53

Inhibition of PKCα (by Go¨6976) in group S showed significantly downregulated expression of IGF1 both at RNA and protein level (RNA: 3.028 ± 0.051 and protein: 4.513 ± 0.20-fold) and absence of IGF1R phosphorylation compared to untreated group S (Fig. 7A–B). On the other hand, PKCδ inhibited (by Rottlerin) D group revealed significant upregulation of IGF1 (mRNA: 3.987 ± 0.17 and protein: 4.644 ± 0.10-fold) and phosphorylated IGF1R (4.513 ± 0.20-fold) compared to untreated group D (Fig. 7A–B).

Phosphorylation status of both Akt and p53 were studied in

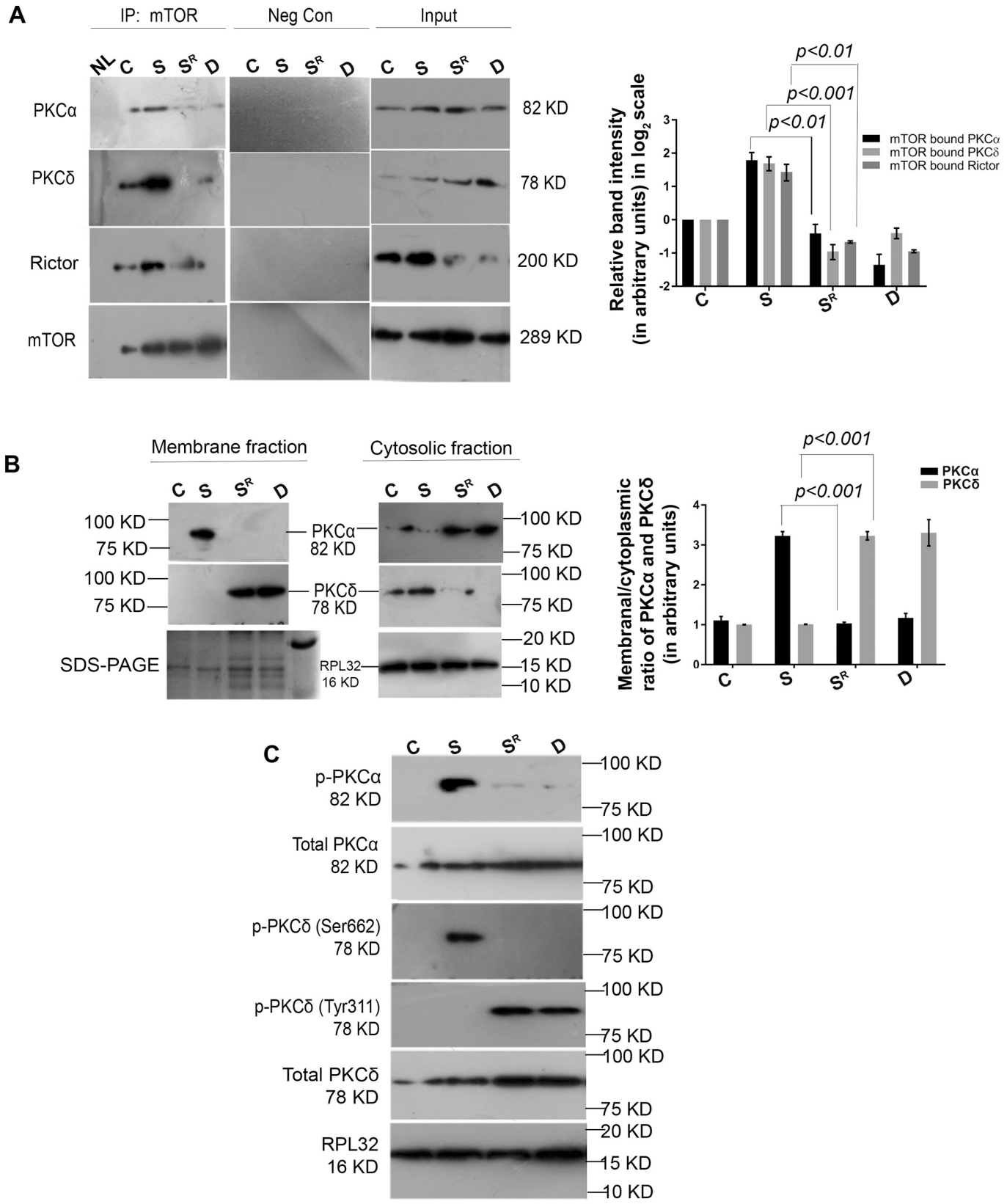

(caption on next page)

respective experimental groups treated with PKC α/δ inhibitors. Phospho Akt (Ser473) was significantly high in PKCδ inhibited group D (2.9 ± 0.045-fold), as observed in group S (Fig. 7C). On the other hand, significant increase in phosphorylated p53 were evident in PKCα inhibited S group (Ser15: 2.967 ± 0.33-fold; Ser46: 3.04 ± 0.52-fold), akin to group D (Fig. 7D).

D group of mice hearts were targeted with p53 siRNA-CMCP abating bystander effects. Successful knocking down of p53 was ascertained by

Fig. 5. mTORC2 differentially regulates PKCα and PKCδ. (A) Co-immunoprecipitation experiments were done using anti-mTOR antibody followed by immunoblotting with anti-PKCα, PKCδ and rictor antibodies. rictor siRNA treatment significantly reduced the binding of PKCα, δ to mTOR in S^R group compared to S. Blots were normalized by immunoblot of mTOR in the same samples. Corresponding graph showing relative level mTOR bound PKCα, δ and rictor in different groups. (B) PKCα and PKCδ also showed differential pattern of translocation to membrane from cytosol among different experimental groups, a major band from a Coomassie blue stained SDS-PAGE gel of fractionated membrane proteins and RPL32 were used as internal loading control for membrane and cytosolic proteins respectively. Corresponding graph showing membrane/cytoplasmic ratio of the same proteins from different experimental groups. (C) Representative western blots showing differential phospho/total status of PKCα and δ among all experimental groups. RPL32 was used as internal loading control. S: exercised mice treated with NS siRNA-CMCP; S^R: exercised mice treated with myocyte targeted rictor siRNA-CMCP; D: detrained mice treated with NS siRNA-CMCP; C: control mice treated with NS siRNA-CMCP. All experiments were repeated independently for three times and the graphs were expressed as mean (±S.E.) of three experiments.

significant downregulated p53 expression in D group hearts compared to NS siRNA-CMCP treated detrained mice group (data not shown). Detrained mice treated with p53siRNA-CMCP, revealed significant upregulation of *igf1* expression (3.265 ± 0.20-fold) compared to NS siRNA-CMCP treated group D comparable with NS siRNA-CMCP treated S group of mice (Fig. 7E). Additionally, ameliorated cardiac function was observed in p53siRNA-CMCP treated detrained mice with markedly decreased LVDD (2.17 ± 0.20 mm), IVST(0.57 ± 0.04 mm) and increased %FS (66.3 ± 5.89%) compared to NS siRNA-CMCP treated group D (LVDD: 3.81 ± 0.15 mm; %FS: 35.9 ± 2.24%; IVST: 0.63 ± 0.08 mm) as revealed by M-mode echocardiographic analysis (Supplementary Fig. 3).

4. Discussion

Loss of cardiac functional efficiency due to exercise cessation is well documented [11,44–46]. Several studies in athletes [13, 14] and in experimental animals [47,46] showed an obvious regression of training-induced cardiac morphological and functional alterations, after withdrawal for short period from active exercise regimen. It was stated that, exercise withdrawal is a major contributing factor for increased susceptibility to cardiovascular diseases in physically inactive athletes [48,49]. A survey on retired National Football League players revealed that Linemen have 52% greater risk of cardiac related death than the general population [50] while another report showed a reduction in cardiovascular functional efficiency after few weeks of detraining in previously trained men [51]. Short-term detraining studies have unanimously pointed towards the trend of decreased maximal oxygen uptake, blood volume, cardiac output, fractional shortening, ejection fraction in human [11,44,52–56] as well as in animal models [19,47,57] as measures of compromised cardiac function. However, the precise molecular mechanism of such maladaptation without any external stress, is poorly understood till date. A previous study from our lab showed that, exercise withdrawal for two weeks resulted in significant deterioration of cardiac function with alteration of activated PKC isoforms in a murine model [19]. Therefore, the present investigation was designed to decipher possible modulators involved in such deterioration of cardiac function upon regimented exercise withdrawal in light of switching from PKCα to PKCδ after detraining. This study focuses on the evidence that, differential level of IGF1 during exercise and detraining is perhaps responsible for conditional activation of specific PKC isoforms (−α to −δ) via intermediate effector molecule mTORC2. It was also evident from this study that downregulation of IGF1 is governed by synergistic activation of PKCδ and deactivation of PKCα, resulting in compromised cardiac condition upon exercise cessation.

Cardiac hypertrophy in both exercised (S) and detrained (D) groups were confirmed by significant increase in HW/BW ratio (Supplementary Fig. 1A), CSA (Supplementary Fig. 1B), hypertrophy markers *anf*, *β-mhc*, *α-mhc*, *serca* (Supplementary Fig. 1D) as described previously [58–60]. Moreover, pathological condition upon exercise cessation was also determined by significantly increased LVDD, IVST and decreased %FS (Supplementary Fig. 1C) corroborating our previous report [19].

Formerly IGF1 had been implicated in exercise-induced cardiac remodelling [22,23] and taken into account to modify maladaptive adrenergic signaling induced by isoproterenol treatment [61]. All these previous findings prompted us initially to probe the status of IGF1 during detraining period. Mature IGF1 binds to IGF1R resulting in trans-autophosphorylation of the cytoplasmic tyrosine kinase domain of the receptor which triggers the activation of downstream canonical pathway [62,63]. In our study, a significant downregulation of IGF1 and phosphorylation of IGF1R were evident in D group (Fig. 1A–B). Gradual decrease in serum IGF1 level was observed in a time point detraining study after exercise, from the 3rd day of detraining till the 15th day (Fig. 1C), which was further substantiated by significant decrease in locally expressed IGF1 and its receptor activation (Fig. 1D). Due to non-availability of enough information involving the direct stimulation of cells *in vitro* to simulate physiological cardiac hypertrophy [64] and non-viable translation of *in vivo* detraining model to *in vitro* models, the use of a novel cardiomyocyte targeted nano-delivery vehicle [39,40] helped us narrow down our observations to myocytes alone in the *in vivo* setup. According to our knowledge, this is the first report of cardiac-specific tissue engineering of certain genes, using a nano-construct for effective monitoring of altered myocardial pathophysiology during exercise and detraining. Cardiac tissue-targeted blocking of IGF1R during exercise (group S^I) and overexpression of IGF1 in detraining condition (group D^{IO}) helped us to dig deep towards underlying mechanism for cardiac morphological, functional alterations as well as differential PKC isoforms activation during exercise and its cessation. Our data revealed that knocking down of IGF1R in swim (S^I) group potentially impaired cardiac function (Fig. 2E), similar to the short-term detrained cardiac condition with decreased %FS, stroke volume and cardiac output as revealed by echocardiography in other reports [51–53,55]. Consistent with the trend, marked increase in HW/BW ratio (Fig. 2C), increased CSA (Fig. 2D), up regulation of pathological hypertrophy markers (Fig. 2F), excess collagen accumulation (Supplementary Fig. 4) were also manifested in S^I group. Interestingly, ameliorated cardiac condition was revealed by IGF1overexpression during exercise cessation in group D^{IO} (Fig. 2C–F, Supplementary Fig. 4). This finding corroborates several earlier studies, where overexpression of IGF1 has been shown to be associated with the betterment of cardiac as well as skeletal muscle [65,66].

Switching of activation of PKCα and PKCδ has been implicated previously in the reversal from physiological to pathological hypertrophy manifestations [19]. In tune with this, phosphorylation (Tyr311) of PKCδ was observed in both S^I and D groups (Fig. 3A) whereas, PKCα (Ser657) phosphorylation was evident in both D^{IO} and S groups (Fig. 3A). Since membrane translocation of PKC is often considered as a surrogate marker for its activation [67,68], exclusive membrane translocation of PKCα (in D^{IO} and S groups) and PKCδ (in S^I and D groups) further corroborated our previous findings (Fig. 3B). Increased phosphorylation of pro-survival kinase Akt which acts downstream of IGF1 and PKCα [69,70], was observed in D^{IO} group similar to group S (Fig. 3C). Since, apoptosis is related with cardiac pathophysiology [40,72] and activated PKCδ had been implied to induce apoptotic markers including p53 [72], caspase-3 [73] and PARP-a substrate for caspase-3 [19,43], the overall apoptotic load in our experimental groups were also checked. Increased expression of total and phosphorylated p53, cleaved fragment of caspase-3 and PARP were evident only in S^I and D groups [Fig. 3D]. So, alteration of the apoptotic markers in cardiomyocytes and increased collagen deposition by cardiac

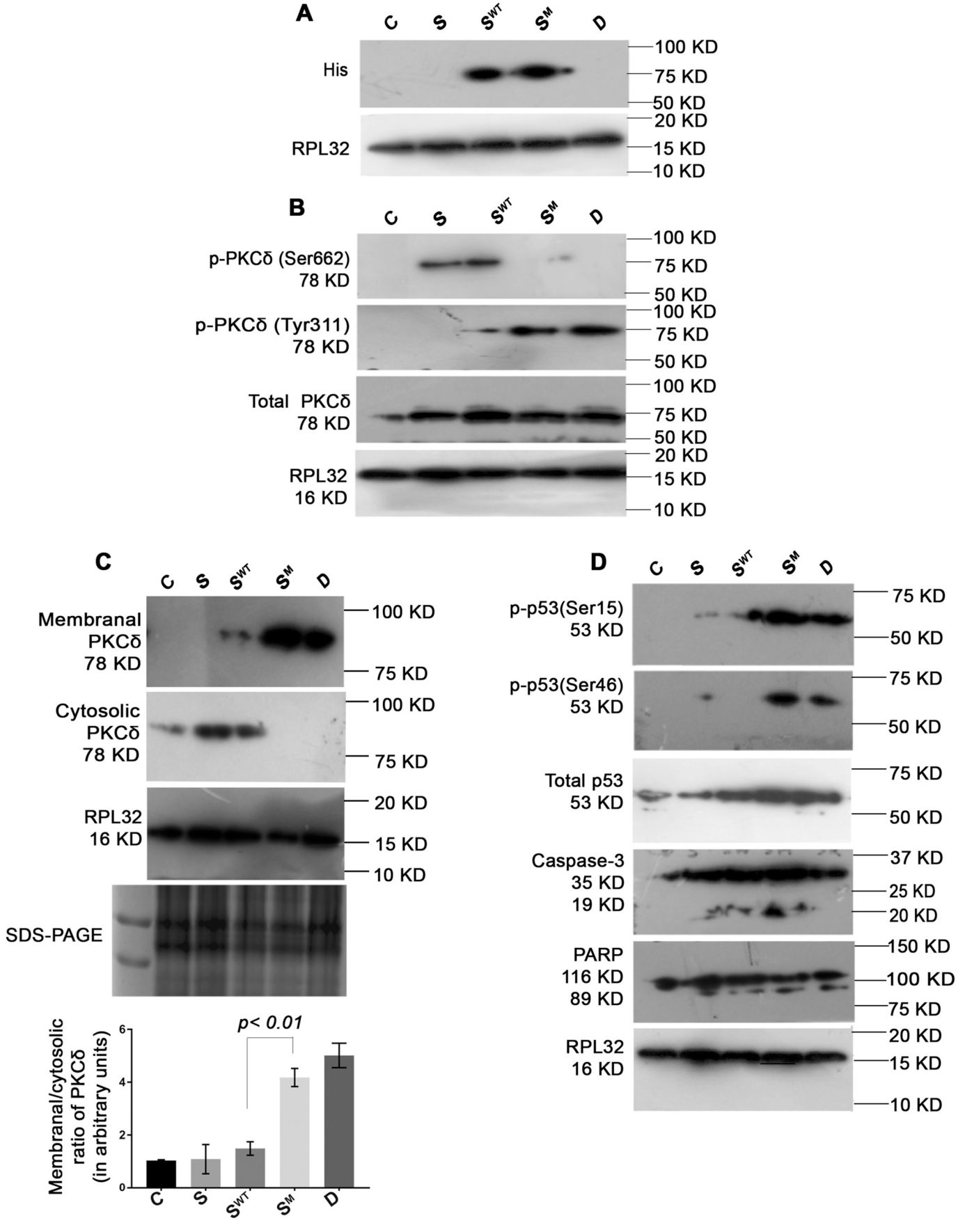

(caption on next page)

Fig. 6. Hydrophobic motif phosphorylation blocks PKCδ activation during exercise. (A) Representative western blot, using anti-his antibody showing successful overexpression of wild type and mutated PKCδ by CMCP-mediated delivery in S^{WT} and S^{M} respectively. RPL32 was used as internal loading control. (B) Representative western blots revealed significantly increased Ser662 phospho/total ratio of PKCδ in S^{WT} compared to either S^{M} or D, while significantly increased Tyr311phospho/total ratio of PKCδ in S^{M} and D compared to S^{WT}. RPL32 was used as internal loading control. (C) Mutated PKCδ showed significantly increased translocation to membrane from cytosol in group S^{M} compared to S^{WT}. A major band from a Coomassie blue stained SDS-PAGE gel of fractionated membrane proteins and RPL32 for cytosolic fraction were used as internal loading control. Corresponding graph showing similar expression pattern of the membranal PKCδ among different experimental groups. (D) Representative western blots showing significantly increased phospho/total p53 (Ser15, Ser46), cleaved Caspase-3 and PARP in S^{M} compared to S^{WT} with RPL32 as internal loading control. S: 4 weeks exercise trained mice treated with empty plasmid-CMCP; S^{WT}: exercised mice treated with myocyte targeted PKCδ wild type-CMCP; S^{M}: exercised mice treated with myocyte targeted mutant PKCδ-CMCP; D: Detrained mice treated with empty plasmid-CMCP; C: control treated with empty plasmid-CMCP. All experiments were repeated independently for three times and the graph was expressed as mean (±S.E.) of three experiments.

connective tissue (Supplementary Fig. 4) were observed in tandem in S^{I} and D groups which are a hallmark for pathological cardiac remodelling [39,41]. Together, all these findings designated that IGF1 might be serving as a potential regulator for differential activation of PKC isoforms during exercise and detraining. To unravel the intricate molecular mechanism of IGF1 mediated PKC switching, status of mTORC2 as a downstream molecule of IGF1/IGF1R mediated pathway [74], was checked. mTORC2 is responsible to maintain ventricular function in pressure overload hypertrophy [75,76]. Our finding revealed downregulated expression of rictor- an mTORC2 obligatory component [33] and mTORC2 specific phosphporylation of mTOR at Ser2481 [77] exclusively in S^{I} group (Fig. 4A), suggesting the association of mTORC2 in IGF1-mediated physiological hypertrophy. Significant restoration of mTORC2 activity was also observed in group D^{IO} similar to group S (Fig. 4A). Myocardium-targeted rictor knockdown in swim group (S^{R}) also manifested severe cardiac deterioration as revealed by M-mode echocardiography (Fig. 4E), with increased HW/BW and CSA (Fig. 4C–D) and upregulated expression of pathological hypertrophy marker genes in S^{R} group (Fig. 4F) corroborating earlier reports that claimed mTORC2 activates its downstream effector molecule Akt [78], which positively regulates physiological cardiac hypertrophy [79]. Activation or inactivation of Akt/mTOR pathway had also been reported to diverge physiological hypertrophy from transverse aortic constriction (TAC) induced pathological condition [80]. Nevertheless, exercise cessation related cardiac deterioration still remained elusive. The role of mTORC2 in PKCα phosphorylation is well documented [34,81]. However, mTORC2 mediated PKCδ phosphorylation and its activation has not been studied extensively. To find out the possible switching mechanism responsible for PKCα to -δ activation during detraining, and to establish the role of mTORC2 in this regard, a co-immunoprecipitation study was undertaken with mTORC2, PKCα and PKCδ. The data revealed a markedly higher interaction between mTORC2::PKCα exclusively in S group (Fig. 5A). Such interaction was responsible for translocation to membrane from cytosol and subsequent activation of PKCα as evidenced by our study (Fig. 5B). Interestingly, interaction between mTORC2 and PKCδ was also evident exclusively in S group (Fig. 5A) but such interaction was not translated into final activation of PKCδ, as translocated PKCδ in the membrane was not found in the aforesaid group (Fig. 5B). Although activated PKCδ was present in both S^{R} and D groups where no interaction was seen between mTORC2 and PKCδ (Fig. 5B).

To understand this quandary, different intermediate phosphorylation statuses were checked. The study revealed that mTORC2 binding to PKCδ might be responsible for its HM (Ser662) phosphorylation resulting in decreased membrane translocation from cytosol and hence deactivation during exercise (Fig. 5B–C). This was partly corroborated by a previous report where it was shown that phosphorylation of PKCδ at Ser662 was regulated by mTORC2 in PDBu-induced HeLa/CP cells [82]. In our study, absence of mTORC2 in both S^{R} and D groups allowed PKCδ to be activated. Activation of PKCs must first be processed by tightly ordered phosphorylation events at three conserved positions: activation loop, hydrophobic motif and turn motif of carboxy-terminal end [83]. Unlike other PKC enzymes, activation loop (Thr505) phosphorylation is not always a precondition for catalytic activity of PKCδ [84,85], whereas Tyr311 phosphorylation is essential for its final activation [83,86], and that depends upon phosphorylation status of hydrophobic motif (Ser662) [86,87]. However, studies have shown that Tyr311 and Thr505 phosphorylate under same condition [85,88]. Since we had checked the status of Thr505 in our previous report [19], here status of Ser662 and Tyr311 were studied. Ser662 was mutated to Alanine in swim group (S^{M}), resulting in higher Tyr311 phosphorylation (Fig. 6B) and subsequent active translocation of PKCδ to membrane compared to group S^{WT} (Fig. 6C). Mutated PKCδ in group S^{M} showed higher apoptotic cardiomyocytes compared to wild type PKCδ (group S^{WT}; Fig. 6D). Thus, S^{M} and D groups exhibited almost similar pattern of PKCδ activation. These results thus imply that dephosphorylated HM might result in activation of PKCδ during detraining. Similar reports suggested that HM phosphorylation counters the activation and membrane translocation of PKCδ [86,87]. The possible explanation was phosphorylated HM elicited a conformational change where the V5 region interacted with the C2-like domain, that masked the C1 domain from being exposed, thus making it less accessible to diacylglycerol (DAG)/phorbol ester [68,85,86]. Mutated HM abrogated the interaction between the V5 region and the C2-like domain, resulting in V5 region unable to mask the C2-like domain. The tightly interacted C1/C2-like domain complex was then more exposed and thus more accessible to DAG which made it more active than the wild type PKCδ. Together all these observations suggest that IGF1 shortfall downregulates mTORC2 activity which in turn activates PKCδ and deactivates PKCα during detraining.

It was still unclear till date whether differentially activated PKC isoforms have any role in the regulation of IGF1 during exercise training and detraining. PKCα has been reported to be a pro-survival protein promoting cell survival via direct activation of Akt [71]. Activated Akt in turn blocks p53 by serving as an antiapoptotic substrate for MDM2 [89,90]. On the other hand, PKCδ is known to phosphorylate and activate p53 [91]. PKCα inhibition during exercise training resulted in Akt dephosphorylation and at the same time, upregulated expression of phosphorylated and total p53, similar to group D (Fig. 7C–D). Blocking of PKCα in group S also lowered the expression of IGF1 at mRNA and protein level (Fig. 7A–B) along with reduced phosphorylation of IGF1R (Fig. 7B), similar to group D. PKCδ inhibition in D group on the other hand, resulted in activation of Akt (Fig. 7C) and deactivated p53 (Fig. 7D) with upregulated expression of IGF1/IGF1R (Fig. 7A–B) similar to group S. However, it required further exploration to unravel precise regulation of IGF1/IGF1R during detraining. Recent studies have revealed that the p53 pathway and IGF1-Akt pathway are involved in sensing and integrating signals arising from intrinsic and extrinsic stress responses and there lies a strong interconnection between them [70, 89]. Our study revealed increased expression of *igf1* in detrained mice hearts treated with p53 siRNA compared to NS-siRNA treated group D (Fig. 7E). This was indicative towards transcriptional repression of *igf1* via p53 during detraining condition. This observation was supported by a previous finding where it was shown that p53/NFYA complex potentially repress basal IGF1 transcription during tumour progression [92]. Moreover, repression of p53 also potentially restored cardiac function even in detraining (Supplementary Fig. 3). Thus, it can be inferred that functionally active p53 suppresses IGF1

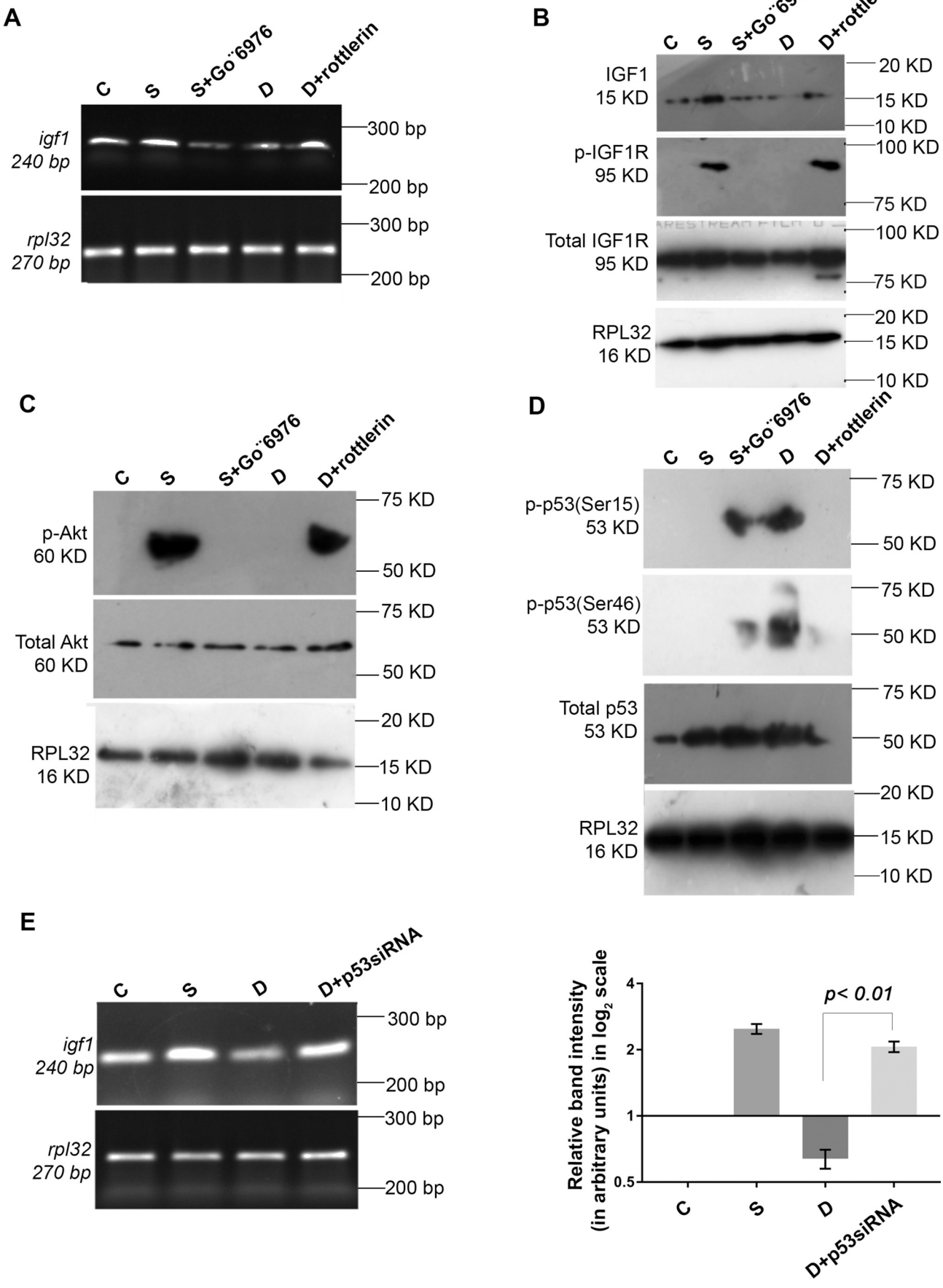

(caption on next page)

Fig. 7. Activated PKCδ and deactivated PKCα downregulate IGF1 via p53 during detraining. (A) RT-PCR analyses revealed significant upregulation of *igf1* in rottlerin treated D group compared to D and downregulation of *igf1* in Go¨6976 treated S group compared to S, *rpl32* was used as internal loading control. (B) Immunoblotting also revealed similar expression pattern of IGF1 and phospho/total IGF1R in different experimental groups. (C) Representative western blot showing significantly higher phosphorylation of Akt in rottlerin treated D group compared to D. (D) Representative western blots revealed significantly increased phospho/total ratio of p53 (Ser 15 and Ser46) in S + Go¨6976 compared to group S. RPL32 was used as internal loading control for all immunoblot experiments. S: PBS treated 4 weeks exercise trained mice; S + Go¨6976: S mice treated with Go¨6976; D: PBS treated detrained mice; D + rottlerin: D mice treated with rottlerin; C: control mice treated with PBS. (E) RT-PCR analysis showing significant upregulation of *igf1* in p53 siRNA-CMCP treated D group compared to group D. *rpl32* was used as internal loading control. Corresponding graphical representation showing expressional changes of *igf1* in different groups; relative mRNA expressions were $\log_2$ transformed S: 4 weeks exercise trained mice treated with NS siRNA-CMCP; D: detrained mice treated with NS siRNA-CMCP; D + p53siRNA: detrained mice treated with myocyte targeted p53siRNA-CMCP; C: control mice treated with NS siRNA-CMCP. All experiments were repeated independently for three times and the graph was expressed as mean (±S.E.) of three experiments.

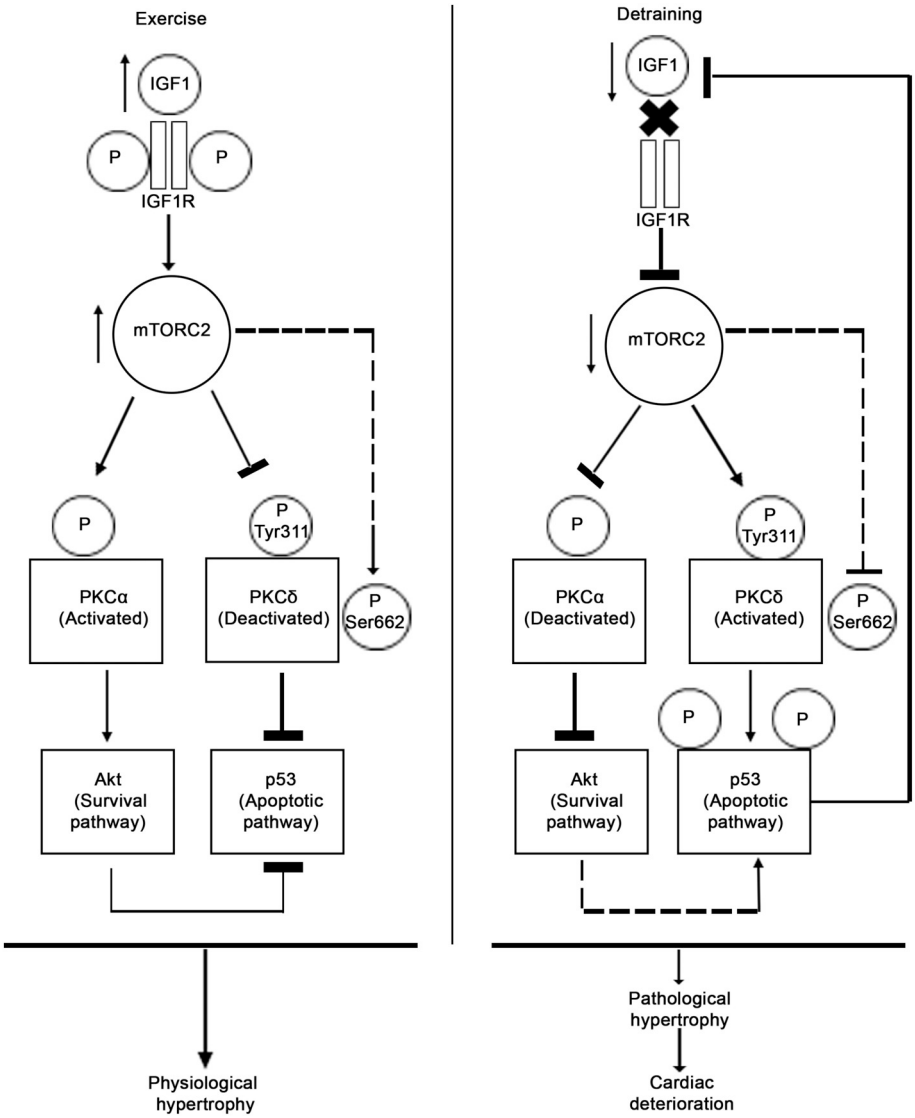

Fig. 8. Schematic representation of a plausible mechanism responsible for the transition of physiologically hypertrophied heart to a maladaptive heart during detraining via differential activation of PKC isoforms (α and δ) involving IGF1/mTORC2/p53.

expression at the level of transcription and continuous shortfall of IGF1/IGF1R/mTORC2 signal ensues deactivation of PKCα and concomitant activation of PKCδ during exercise withdrawal. It could thus be suggested that a lesser level of physical activity or sequential detraining might be recommended to maintain cardiac health of athletes post retirement.

5. Conclusion

Our study distinctly demonstrates that reduced level of IGF1during short-term detraining diminishes mTORC2 mediated differential regulation of PKC isoforms (α and δ). Deactivated PKCα and activated PKCδ together downregulate IGF1 via p53, which in turn results in induced apoptosis and compromised cardiac condition. Thus, a feedback loop exists between IGF1 and p53 which senses the presence of differentially activated PKC isoforms (Fig. 8). According to our knowledge, this is the first *in vivo* study to comprehensively investigate the intricate molecular mechanisms responsible for cardiac maladaptation without any external agonists, during detraining period.

Supplementary data to this article can be found online at https://doi.org/10.1016/j.bbadis.2019.07.003.

Author contributions

SS conceived and designed the idea of the project. EC conducted the experiments, analysed the results and wrote the manuscript with SS. RDC assisted in conducting most experiments and preparing the manuscript.

Transparency document

The Transparency document associated with this article can be found, in online version.

Declaration of Competing Interest

No conflict of interest to disclose.

Acknowledgement

This work was funded by Department of Biotechnology (Grant numbers: BT-PR3709/BRB/10/980/2011 and BT/PR7016/NNT/28/641/2012), Department of Science and Technology (Grant number: SB/SO/HS-148/2013) to Dr. S. Sarkar and DST-FIST program (Sanction number: SR/FST/LS-II/2017/110), Government of India; E. Chatterjee was supported by fellowship from Indian Council of Medical Research (Sanction number 3/1/2(9)/CVD/2018-NCD-II).

References

[1] J.N. Morris, R. Pollard, M.G. Everitt, S.P.W. Chave, A.M. Semmence, Vigorous exercise in leisure-time: protection against coronary heart disease, Lancet 316 (8206) (1980) 1207–1210.
[2] J.M. Hagberg, J.J. Park, M.D. Brown, The role of exercise training in the treatment of hypertension, Sports Med. 30 (3) (2000) 193–206.
[3] B.K. Pedersen, C.P. Fischer, Beneficial health effects of exercise–the role of IL-6 as a myokine, Trends Pharmacol. Sci. 28 (4) (2007) 152–156.
[4] C. Handschin, B.M. Spiegelman, The role of exercise and PGC1α in inflammation and chronic disease, Nature *454* (7203) (2008) 463.
[5] G.M. Ellison, C.D. Waring, C. Vicinanza, D. Torella, Physiological cardiac remodelling in response to endurance exercise training: cellular and molecular mechanisms, Heart 98 (1) (2012) 5–10.
[6] L. Tao, Y. Bei, S. Lin, H. Zhang, Y. Zhou, J. Jiang, P. Chen, S. Shen, J. Xiao, X. Li, Exercise training protects against acute myocardial infarction via improving myocardial energy metabolism and mitochondrial biogenesis, Cell. Physiol. Biochem. 37 (1) (2015) 162–175.
[7] S. Sharma, A. Merghani, L. Mont, Exercise and the heart: the good, the bad, and the ugly, Eur. Heart J. 36 (23) (2015) 1445–1453.
[8] T. Luijkx, M.J. Cramer, N.H. Prakken, C.F. Buckens, A. Mosterd, R. Rienks, F.J. Backx, P.T.M. Willem, B.K. Velthuis, Sport category is an important determinant of cardiac adaptation: an MRI study, Br. J. Sports Med. 46 (16) (2012) 1119–1124.
[9] T. Radovits, A. Oláh, Á. Lux, B.T. Németh, L. Hidi, E. Birtalan, D. Kellermayer, C. Mátyás, G. Szabó, B. Merkely, Rat model of exercise-induced cardiac hypertrophy: hemodynamic characterization using left ventricular pressure-volume analysis, Am. J. Phys. Heart Circ. Phys. 305 (1) (2013) H124–H134.
[10] F.S. Evangelista, P.C. Brum, J.E. Krieger, Duration-controlled swimming exercise training induces cardiac hypertrophy in mice, Braz. J. Med. Biol. Res. 36 (12) (2003) 1751–1759.
[11] I. Mujika, S. Padilla, Detraining: loss of training-induced physiological and performance adaptations, Part I. *Sports Medicine* 30 (2) (2000) 79–87.
[12] I. Esain, S.M. Gil, I. Bidaurrazaga-Letona, A. Rodriguez-Larrad, Effects of 3 months of detraining on functional fitness and quality of life in older adults who regularly exercise, *Aging clinical and experimental research*, pp. (2018) 1–8.
[13] A. Pelliccia, B.J. Maron, R. De Luca, F.M. Di Paolo, A. Spataro, F. Culasso, Remodeling of left ventricular hypertrophy in elite athletes after long-term deconditioning, Circulation 105 (8) (2002) 944–949.
[14] B.J. Maron, A. Pelliccia, A. Spataro, M. Granata, Reduction in left ventricular wall thickness after deconditioning in highly trained Olympic athletes, Heart 69 (2) (1993) 125–128.
[15] G. Pavlik, N. Bachl, W. Wollein, Effect of training and detraining on the resting echocardiographic parameters in runners and cyclists, International Journal of Sports Cardiology 3 (1) (1986) 35–45.
[16] R.M. Bell, D.J. Burns, Lipid activation of protein kinase C, J. Biol. Chem. 266 (8) (1991) 4661–4664.
[17] Y. Koide, K. Tamura, A. Suzuki, K. Kitamura, K. Yokoyama, T. Hashimoto, N. Hirawa, M. Kihara, S. Umemura, Differential induction of protein kinase C isoforms at the cardiac hypertrophy stage and congestive heart failure stage in Dahl salt-sensitive rats, Hypertens. Res. 26 (5) (2003) 421–426.
[18] P. Sil, V. Kandaswamy, S. Sen, Increased protein kinase C activity in myotrophin-induced myocyte growth, Circ. Res. 82 (11) (1998) 1173–1188.
[19] S. Naskar, K. Datta, A. Mitra, K. Pathak, R. Datta, T. Bansal, S. Sarkar, Differential and conditional activation of PKC-isoforms dictates cardiac adaptation during physiological to pathological hypertrophy, PloS one *9* (8) (2014) e104711.
[20] M. Arcopinto, E. Bobbio, E. Bossone, P. Perrone-Filardi, R. Napoli, L. Sacca, A. Cittadini, The GH/IGF-1 axis in chronic heart failure, Endocrine, Metabolic & Immune Disorders-Drug Targets (Formerly Current Drug Targets-Immune, Endocrine & Metabolic Disorders) 13 (1) (2013) 76–91.
[21] R. Troncoso, C. Ibarra, J.M. Vicencio, E. Jaimovich, S. Lavandero, New insights into IGF-1 signaling in the heart, Trends in Endocrinology & Metabolism 25 (3) (2014) 128–137.
[22] J. Kim, A.R. Wende, S. Sena, H.A. Theobald, J. Soto, C. Sloan, B.E. Wayment, S.E. Litwin, M. Holzenberger, D. LeRoith, E.D. Abel, Insulin-like growth factor I receptor signaling is required for exercise-induced cardiac hypertrophy, Mol. Endocrinol. 22 (11) (2008) 2531–2543.
[23] J.R. McMullen, T. Shioi, W.Y. Huang, L. Zhang, O. Tarnavski, E. Bisping, M. Schinke, S. Kong, M.C. Sherwood, J. Brown, L. Riggi, The insulin-like growth factor 1 receptor induces physiological heart growth via the phosphoinositide 3-kinase (p110α) pathway, J. Biol. Chem 279 (6) (2004) 4782–4793.
[24] J.R. McMullen, Role of insulin-like growth factor 1 and phosphoinositide 3-kinase in a setting of heart disease, Clin. Exp. Pharmacol. Physiol. 35 (3) (2008) 349–354.
[25] K.L. Weeks, J.R. McMullen, The athlete's heart vs. the failing heart: can signaling explain the two distinct outcomes? Physiology 26 (2) (2011) 97–105.
[26] Y. Higashi, S. Sukhanov, A. Anwar, S.Y. Shai, P. Delafontaine, Aging, atherosclerosis, and IGF-1, Journals of Gerontology Series A: Biomedical Sciences and Medical Sciences 67 (6) (2012) 626–639.
[27] A. Pecherskaya, M. Solem, IGF1 activates PKC α-dependent protein synthesis in adult rat cardiomyocytes, Molecular Cell Biology Research Communications 4 (3) (2000) 166–171.
[28] M. Sandri, L. Barberi, A.Y. Bijlsma, B. Blaauw, K.A. Dyar, G. Milan, C. Mammucari, C.G.M. Meskers, G. Pallafacchina, A. Paoli, D. Pion, Signalling pathways regulating muscle mass in ageing skeletal muscle. The role of the IGF1-Akt-mTOR-FoxO pathway, Biogerontology 14 (3) (2013) 303–323.
[29] C. Rommel, S.C. Bodine, B.A. Clarke, R. Rossman, L. Nunez, T.N. Stitt, G.D. Yancopoulos, D.J. Glass, Mediation of IGF-1-induced skeletal myotube hypertrophy by PI (3) K/Akt/mTOR and PI (3) K/Akt/GSK3 pathways, Nature cell biology *3* (11) (2001) 1009.
[30] D.H. Kim, D.D. Sarbassov, S.M. Ali, J.E. King, R.R. Latek, H. Erdjument-Bromage, P. Tempst, D.M. Sabatini, mTOR interacts with raptor to form a nutrient-sensitive complex that signals to the cell growth machinery, Cell 110 (2) (2002) 163–175.
[31] K. Hara, Y. Maruki, X. Long, K.I. Yoshino, N. Oshiro, S. Hidayat, C. Tokunaga, J. Avruch, K. Yonezawa, Raptor, a binding partner of target of rapamycin (TOR), mediates TOR action, Cell 110 (2) (2002) 177–189.
[32] I. Bracho-Valdés, P. Moreno-Alvarez, I. Valencia-Martínez, E. Robles-Molina, L. Chávez-Vargas, J. Vázquez-Prado, mTORC1-and mTORC2-interacting proteins keep their multifunctional partners focused, IUBMB Life 63 (10) (2011) 896–914.
[33] D.D. Sarbassov, S.M. Ali, D.H. Kim, D.A. Guertin, R.R. Latek, H. Erdjument-Bromage, P. Tempst, D.M. Sabatini, Rictor, a novel binding partner of mTOR, defines a rapamycin-insensitive and raptor-independent pathway that regulates the cytoskeleton, Curr. Biol. 14 (14) (2004) 1296–1302.
[34] D.A. Guertin, D.M. Stevens, C.C. Thoreen, A.A. Burds, N.Y. Kalaany, J. Moffat, M. Brown, K.J. Fitzgerald, D.M. Sabatini, Ablation in mice of the mTORC components raptor, rictor, or mLST8 reveals that mTORC2 is required for signaling to Akt-FOXO and PKCα, but not S6K1, Dev. Cell 11 (6) (2006) 859–871.
[35] D.D. Sarbassov, D.A. Guertin, S.M. Ali, D.M. Sabatini, Phosphorylation and regulation of Akt/PKB by the rictor-mTOR complex, Science 307 (5712) (2005) 1098–1101.
[36] C.L. Galindo, M.A. Skinner, M. Errami, L.D. Olson, D.A. Watson, J. Li, J.F. McCormick, L.J. McIver, N.M. Kumar, T.Q. Pham, H.R. Garner, Transcriptional profile of isoproterenol-induced cardiomyopathy and comparison to exercise-induced cardiac hypertrophy and human cardiac failure, BMC physiology *9* (1) (2009) 23.
[37] S. Sen, R.C. Tarazi, P.A. Khairallah, F.M. Bumpus, Cardiac hypertrophy in spontaneously hypertensive rats, Circ. Res. 35 (5) (1974) 775–781.
[38] R. Datta, T. Bansal, S. Rana, K. Datta, S. Chattopadhyay, M. Chawla-Sarkar, S. Sarkar, Hsp90/Cdc37 assembly modulates TGFβ receptor-II to act as a profibrotic regulator of TGFβ signaling during cardiac hypertrophy, Cell. Signal. 27 (12) (2015) 2410–2424.
[39] S. Rana, K. Datta, T.L. Reddy, E. Chatterjee, P. Sen, M. Pal-Bhadra, U. Bhadra, A. Pramanik, P. Pramanik, M. Chawla-Sarkar, S. Sarkar, A spatio-temporal cardiomyocyte targeted vector system for efficient delivery of therapeutic payloads to regress cardiac hypertrophy abating bystander effect, J. Control. Release 200 (2015) 167–178.
[40] S. Rana, R. Datta, R.D. Chaudhuri, E. Chatterjee, M. Chawla-Sarkar, S. Sarkar, Nanotized PPARα Overexpression Targeted to Hypertrophied Myocardium Improves Cardiac Function by Attenuating the p53-GSK3β-Mediated Mitochondrial Death Pathway, Antioxid. Redox Signal. 30 (5) (2019) 713–732.
[41] S.A. Mir, A. Chatterjee, A. Mitra, K. Pathak, S.K. Mahata, S. Sarkar, Inhibition of signal transducer and activator of transcription 3 (STAT3) attenuates interleukin-6 (IL-6)-induced collagen synthesis and resultant hypertrophy in rat heart, J. Biol. Chem. 287 (4) (2012) 2666–2677.
[42] S. Sarkar, E. Vellaichamy, D. Young, S. Sen, Influence of cytokines and growth factors in ANG II-mediated collagen upregulation by fibroblasts in rats: role of myocytes, Am. J. Phys. Heart Circ. Phys. 287 (1) (2004) H107–H117.
[43] A. Chatterjee, S.A. Mir, D. Dutta, A. Mitra, K. Pathak, S. Sarkar, Analysis of p53 and

NF-κB signaling in modulating the cardiomyocyte fate during hypertrophy, J. Cell. Physiol. 226 (10) (2011) 2543–2554.
[44] I. MUJIKA, S. PADILLA, Cardiorespiratory and metabolic characteristics of detraining in humans, Med. Sci. Sports Exerc. 33 (3) (2001) 413–421.
[45] D. Agarwal, R.B. Dange, J. Vila, A.J. Otamendi, J. Francis, Detraining differentially preserved beneficial effects of exercise on hypertension: effects on blood pressure, cardiac function, brain inflammatory cytokines and oxidative stress, PLoS One 7 (12) (2012) e52569.
[46] A. Oláh, D. Kellermayer, C. Mátyás, B.T. Németh, Á. Lux, L. Szabó, M. Török, M. Ruppert, A. Meltzer, A.A. Sayour, K. Benke, Complete reversion of cardiac functional adaptation induced by exercise training, Med. Sci. Sports Exerc. 49 (3) (2017) 420–429.
[47] D.S. Bocalini, E.V. Carvalho, A.F. de Sousa, R.F. Levy, P.J. Tucci, Exercise training-induced enhancement in myocardial mechanics is lost after 2 weeks of detraining in rats, Eur. J. Appl. Physiol. 109 (2010) 909–914.
[48] R.T. Hurst, R.F. Burke, E. Wissner, A. Roberts, C.B. Kendall, S.J. Lester, V. Somers, M.E. Goldman, Q. Wu, B. Khandheria, Incidence of subclinical atherosclerosis as a marker of cardiovascular risk in retired professional football players, Am. J. Cardiol. 105 (8) (2010) 1107–1111.
[49] S. Witkowski, E.E. Spangenburg, Reduced physical activity and the retired athlete: a dangerous combination? Br. J. Sports Med. 42 (12) (2008) 952–953.
[50] S. Baron, R. Rinsky, NIOSH Mortality Study of NFL Football Players: 1959–1988, Centers for Disease Control, National Institute of Occupational Safety and Health, Cincinnati, OH, 1994 88–85.
[51] E.F. Coyle, M.K. Hemmert, A.R. Coggan, Effects of detraining on cardiovascular responses to exercise: role of blood volume, J. Appl. Physiol. 60 (1) (1986) 95–99.
[52] M.S. Nugroho, M. Or, The Detraining Effects of Complete Inactivity, Doctoral dissertation, Thesis, 2005.
[53] M. Javad, M. Mohammadali, K. Toba, The effect of aerobic continuous training and detraining on left ventricular structure and function in male students, Physical education of students 21 (2) (2017) 61–65.
[54] P. Nolan, S. Keeling, C. Robitaille, C. Buchanan, L. Dalleck, The effect of detraining after a period of training on cardiometabolic health in previously sedentary individuals, International Journal of Environmental Research and Public Health 15 (10) (2018) 2303.
[55] E.F. Coyle, W.H. Martin 3rd, D.R. Sinacore, M.J. Joyner, J.M. Hagberg, J.O. Holloszy, Time course of loss of adaptations after stopping prolonged intense endurance training, J. Appl. Physiol. 57 (6) (1984) 1857–1864.
[56] P.D. Neufer, The effect of detraining and reduced training on the physiological adaptations to aerobic exercise training, Sports Med. 8 (5) (1989) 302–320.
[57] O.J. Kemi, P.M. Haram, U. Wisløff, Ø. Ellingsen, Aerobic fitness is associated with cardiomyocyte contractile capacity and endothelial function in exercise training and detraining, Circulation 109 (23) (2004) 2897–2904.
[58] A. Mitra, T. Basak, K. Datta, S. Naskar, S. Sengupta, et al., Role of a crystallinB as a regulatory switch in modulating cardiomyocyte apoptosis by mitochondria or endoplasmic reticulum during cardiac hypertrophy and myocardial infarction, Cell Death Dis. 4 (2013) e582.
[59] K.L. Vikstrom, T. Bohlmeyer, S.M. Factor, L.A. Leinwand, Hypertrophy, pathology, and molecular markers of cardiac pathogenesis, Circ. Res. 82 (7) (1998) 773–778.
[60] J.R. McMullen, T. Shioi, L. Zhang, O. Tarnavski, M.C. Sherwood, P.M. Kang, S. Izumo, Phosphoinositide 3-kinase (p110α) plays a critical role for the induction of physiological, but not pathological, cardiac hypertrophy, Proc. Natl. Acad. Sci. 100 (21) (2003) 12355–12360.
[61] S.R. Roof, J. Boslett, D. Russell, C. Rio, J. Alecusan, J.L. Zweier, M.T. Ziolo, R. Hamlin, P.J. Mohler, J. Curran, Insulin-like growth factor 1 prevents diastolic and systolic dysfunction associated with cardiomyopathy and preserves adrenergic sensitivity, Acta Physiol. 216 (4) (2016) 421–434.
[62] A. Philippou, M. Maridaki, S. Pneumaticos, M. Koutsilieris, The complexity of the IGF1 gene splicing, posttranslational modification and bioactivity, Molecular Medicine 20 (1) (2014) 202.
[63] J.M. Kavran, J.M. McCabe, P.O. Byrne, M.K. Connacher, Z. Wang, A. Ramek, S. Sarabipour, Y. Shan, D.E. Shaw, K. Hristova, P.A. Cole, How IGF-1 activates its receptor, Elife 3 (2014).
[64] D.J. Youtz, M.C. Isfort, C.M. Eichenseer, T.D. Nelin, L.E. Wold, In vitro effects of exercise on the heart, Life Sci. 116 (2) (2014) 67–73.
[65] A.M. Samarel, IGF-1 overexpression rescues the failing heart, Circ.Res 90 (6) (2002) 631–633.
[66] F. Ye, S. Mathur, M. Liu, S.E. Borst, G.A. Walter, H.L. Sweeney, K. Vandenborne, Overexpression of insulin-like growth factor-1 attenuates skeletal muscle damage and accelerates muscle regeneration and functional recovery after disuse, Exp. Physiol. 98 (5) (2013) 1038–1052.
[67] J.A. Matthews, M. Acevedo-Duncan, R.L. Potter, Selective decrease of membrane-associated PKC-α and PKC-ε in response to elevated intracellular O-GlcNAc levels in transformed human glial cells, Biochimica et Biophysica Acta (BBA)-Molecular Cell Research 1743 (3) (2005) 305–315.
[68] S.F. Steinberg, Distinctive activation mechanisms and functions for protein kinase Cδ, Biochem. J. 384 (3) (2004) 449–459.
[69] T.N. Stitt, D. Drujan, B.A. Clarke, F. Panaro, Y. Timofeyva, W.O. Kline, M. Gonzalez, G.D. Yancopoulos, D.J. Glass, The IGF-1/PI3K/Akt pathway prevents expression of muscle atrophy-induced ubiquitin ligases by inhibiting FOXO transcription factors, Mol. Cell 14 (3) (2004) 395–403.
[70] C. Partovian, M. Simons, Regulation of protein kinase B/Akt activity and Ser473 phosphorylation by protein kinase Cα in endothelial cells, Cell. Signal. 16 (8) (2004) 951–957.
[71] R. Shannon, M. Chaudhry, Effect of α1-adrenergic receptors in cardiac pathophysiology, Am. Heart J. 152 (5) (2006) 842–850.
[72] T. Abbas, D. White, L. Hui, K. Yoshida, D.A. Foster, J. Bargonetti, Inhibition of human p53 basal transcription by down-regulation of protein kinase Cδ, J. Biol. Chem. 279 (11) (2004) 9970–9977.
[73] Y.F. Liao, Y.C. Hung, W.H. Chang, G.J. Tsay, T.C. Hour, H.C. Hung, G.Y. Liu, The PKC delta inhibitor, rottlerin, induces apoptosis of haematopoietic cell lines through mitochondrial membrane depolarization and caspases' cascade, Life Sci. 77 (6) (2005) 707–719.
[74] N. Cybulski, P. Polak, J. Auwerx, M.A. Rüegg, M.N. Hall, mTOR complex 2 in adipose tissue negatively controls whole-body growth, Proc. Natl. Acad. Sci. 106 (24) (2009) 9902–9907.
[75] P. Shende, L. Xu, C. Morandi, L. Pentassuglia, P. Heim, S. Lebboukh, C. Berthonneche, T. Pedrazzini, B.A. Kaufmann, M.N. Hall, M.A. Rüegg, Cardiac mTOR complex 2 preserves ventricular function in pressure-overload hypertrophy, Cardiovasc. Res. 109 (1) (2015) 103–114.
[76] S. Balasubramanian, R.K. Johnston, P.C. Moschella, S.K. Mani, J. Tuxworth, J. William, D. Kuppuswamy, mTOR in growth and protection of hypertrophying myocardium, Cardiovascular & Hematological Agents in Medicinal Chemistry (Formerly Current Medicinal Chemistry-Cardiovascular & Hematological Agents) 7 (1) (2009) 52–63.
[77] J. Copp, G. Manning, T. Hunter, TORC-specific phosphorylation of mammalian target of rapamycin (mTOR): phospho-Ser2481 is a marker for intact mTOR signaling complex 2, Cancer Res. 69 (5) (2009) 1821–1827.
[78] D.M. Sabatini, mTOR and cancer: insights into a complex relationship, Nature Reviews Cancer 6 (9) (2006) 729.
[79] B. DeBosch, I. Treskov, T.S. Lupu, C. Weinheimer, A. Kovacs, M. Courtois, A.J. Muslin, Akt1 is required for physiological cardiac growth, Circulation 113 (17) (2006) 2097–2104.
[80] O.J. Kemi, M. Ceci, U. Wisloff, S. Grimaldi, P. Gallo, G.L. Smith, G. Condorelli, O. Ellingsen, Activation or inactivation of cardiac Akt/mTOR signaling diverges physiological from pathological hypertrophy, J. Cell. Physiol. 214 (2) (2008) 316–321.
[81] T. Ikenoue, K. Inoki, Q. Yang, X. Zhou, K.L. Guan, Essential function of TORC2 in PKC and Akt turn motif phosphorylation, maturation and signalling, EMBO J. 27 (14) (2008) 1919–1931.
[82] A. Basu, S. Sridharan, S. Persaud, Regulation of protein kinase Cδ downregulation by protein kinase Cε and mammalian target of rapamycin complex 2, Cell. Signal. 21 (11) (2009) 1680–1685.
[83] M. Freeley, D. Kelleher, A. Long, Regulation of protein kinase C function by phosphorylation on conserved and non-conserved sites, Cell. Signal. 23 (5) (2011) 753–762.
[84] L. Stempka, A. Girod, H.J. Müller, G. Rincke, F. Marks, M. Gschwendt, D. Bossemeyer, Phosphorylation of protein kinase Cδ (PKCδ) at threonine 505 is not a prerequisite for enzymatic activity expression of rat PKCδ and an alanine 505 mutant in bacteria in a functional form, J. Biol. Chem. 272 (10) (1997) 6805–6811.
[85] S.F. Steinberg, Structural basis of protein kinase C isoform function, Physiol. Rev. 88 (4) (2008) 1341–1378.
[86] M.B. Karmacharya, J.I. Jang, Y.J. Lee, Y.S. Lee, J.W. Soh, Mutation of the hydrophobic motif in a phosphorylation-deficient mutant renders protein kinase C delta more apoptotically active, Arch. Biochem. Biophys. 493 (2) (2010) 242–248.
[87] X. Feng, K.P. Becker, S.D. Stribling, K.G. Peters, Y.A. Hannun, Regulation of receptor-mediated protein kinase C membrane trafficking by autophosphorylation, J. Biol. Chem. 275 (22) (2000) 17024–17034.
[88] V.O. Rybin, J. Guo, A. Sabri, H. Elouardighi, E. Schaefer, S.F. Steinberg, Stimulus-specific differences in protein kinase Cδ localization and activation mechanisms in cardiomyocytes, J. Biol. Chem. 279 (18) (2004) 19350–19361.
[89] Z. Feng, p53 regulation of the IGF-1/AKT/mTOR pathways and the endosomal compartment, Cold Spring Harbor perspectives in biology 2 (2) (2010) a001057.
[90] A.J. Levine, Z. Feng, T.W. Mak, H. You, S. Jin, Coordination and communication between the p53 and IGF-1–AKT–TOR signal transduction pathways, Genes Dev. 20 (3) (2006) 267–275.
[91] N. Dashzeveg, K. Yoshida, Crosstalk between tumor suppressors p53 and PKCδ:execution of the intrinsic apoptotic pathways, Cancer Lett. 377 (2) (2016) 158–163.
[92] E.M. Goetz, B. Shankar, Y. Zou, J.C. Morales, X. Luo, S. Araki, R. Bachoo, L.D. Mayo, D.A. Boothman, ATM-dependent IGF-1 induction regulates secretory clusterin expression after DNA damage and in genetic instability, Oncogene 30 (35) (2011) 3745.